New insights into chloromethyl-oxirane and chloromethyl-thiirane in liquid and solid phase from low-temperature infrared spectroscopy and ab initio modeling

O. Palumbo, A. Paolone, M. Campetella, F. Ramondo, F. Cappelluti, L. Gontrani

PII: S1386-1425(20)31040-4

DOI: https://doi.org/10.1016/j.saa.2020.119061

Reference: SAA 119061

To appear in: *Spectrochimica Acta Part A: Molecular and Biomolecular Spectroscopy*

Received date: 5 June 2020

Revised date: 2 October 2020

Accepted date: 6 October 2020

Please cite this article as: O. Palumbo, A. Paolone, M. Campetella, et al., New insights into chloromethyl-oxirane and chloromethyl-thiirane in liquid and solid phase from low-temperature infrared spectroscopy and ab initio modeling, *Spectrochimica Acta Part A: Molecular and Biomolecular Spectroscopy* (2020), https://doi.org/10.1016/j.saa.2020.119061

New insights into chloromethyl-oxirane and chloromethyl-thiirane in liquid and solid phase from low-temperature infrared spectroscopy and *ab initio* modeling

O. Palumbo, A. Paolone
CNR-ISC, UOS La Sapienza, P. le A. Moro 5, 00185 Roma (Italy)

M. Campetella, F. Ramondo
Dipartimento di Chimica, Università degli Studi di Roma, P. le Aldo Moro 5, 00185 Roma (Italy)

F. Cappelluti*
Dipartimento di Ingegneria e Scienza dell'Informazione e Matematica, Università dell'Aquila, Via Vetoio 5, Coppito, 67100 L'Aquila (Italy)

L. Gontrani*
Dipartimento di Ingegneria Industriale, Università di Roma "Tor Vergata", Viale degli ingegneri, I-00133 Roma (Italy)

Abstract

A detailed study of the conformational landscape of chloromethyl-oxirane and chloromethyl-thiirane is here reported. The equilibrium of the three different conformers of the two molecules was assessed, using a joint approach of experimental and theoretical methods. High quality infrared spectroscopy measurements of the liquid and of the crystalline phases were interpreted with the aid of *ab initio* Molecular Dynamics (AIMD) simulations, anharmonic frequencies and free energy calculations, obtaining a very good reproduction of the experimental data. The modulation of the conformational equilibrium upon the addition of polar and non-polar solvents was computationally evaluated and results found a confirmation in experimental measures.

* Author for correspondence:
francesco.cappelluti@graduate.univaq.it
lorenzo.gontrani@uniroma2.it

INTRODUCTION

The conformational stability of chloromethyl-oxirane C_3H_5ClO and chloromethyl-thiirane C_3H_5ClS (traditionally known as epichlorohydrin and epithiochlorohydrin and sometimes abbreviated as ClMO and ClMT) has been matter of several investigations in the respective gas and condensed states [1-4], and a wide number of studies is therefore nowadays available. Both compounds possess three conformers, generated by the rotation around the C-C bond connecting the chloromethyl group and the three-membered ring: *gauche-1*, *gauche-2* and *cis*. For both the isolated molecules, the relative abundance of the three forms is *gauche-2*>*gauche-1*>*cis*. Raman spectroscopy measurements of liquid chloromethyl-oxirane established that the polar *gauche-1* and *cis* conformers gain stability in the condensed state with respect to the *gauche-2* conformer. More precisely, the polar *gauche-1* form of chloromethyl-oxirane is predominant in the liquid phase where the *cis* form is slightly more stable than *gauche-2*. Moreover, *gauche-1* is the only form in the solid. This behavior was explained claiming hydrogen bonding stabilization in the condensed phases, owing to the large dipole moment associated with this conformation. Evidently, on these premises, the less polar *gauche-2* conformer is actually expected to be the predominant component in the gas phase, as well as in liquid xenon solution at cryogenic temperature.
Concerning chloromethyl-thiirane, one has first to remark that the presence of sulphur atom instead of an oxygen one might exert effects on the stability and population of the three possible conformers. It was definitively proved that the *gauche 2* conformer largely predominates over the *gauche-1* form in the gas phase and in very low temperature liquid xenon. It was also established that the solid consists of a unique form, that is the *gauche-2* conformer, and that the liquid state is a mixture of the two *gauche* conformers.
In the most recent work [4], the occurrence of the three possible conformers of the molecules in their liquid phase was successfully estimated from X-ray diffraction, AIMD and infrared spectroscopy methods and the results would seem to suggest a conclusive re-examination of the topic. Indeed, we now wish to accomplish the study of these two interesting systems reconsidering the whole matter in the light of infrared and far infrared spectroscopy for the liquid and solid phases of chloromethyl-oxirane and chloromethyl-thiirane, performed in a wide and suitable temperature range. The effect of the chemical environment, that is the polarity of the solvent, on the conformational population is a further aspect of the investigation we have examined. The whole matter is supported by computational simulations based on Density Functional Theory and Gaussian-4 method calculations providing infrared spectra, stability considerations and conformational populations, along with their temperature dependence.

EXPERIMENTAL DETAILS

The infrared spectroscopy measurements were performed by means of a Bruker IFS125 HR spectrometer at the AILES beamline of the SOLEIL Synchrotron in the frequency range between 50 and 5000 cm^{-1} [5, 6]. In the region below 680 cm^{-1} we used a 6 μm Mylar beamsplitter, a globar source and a bolometer detector; above 600 cm^{-1} a KBr beamsplitter, a globar source and a MCT detector were used; for both ranges the spectral resolution was 0.5 cm^{-1}. Thin layers of liquids around 6μm-and 15 μm-thick for medium-infrared (MIR) and far-infrared (FIR) measurements, respectively, were placed between two diamond windows of a vacuum tight cell. The transmission was calculated using the spectrum of the bare optical windows as a reference. Transmission measurements were converted to absorbance data. All measurements were performed in high vacuum ($P < 10^{-4}$ mbar), in order to avoid contaminations from water and carbon dioxide. The data were collected on cooling the samples down to 160 K by means of a Cryomech Cryopump with a

temperature rate of 5 K/min.
The samples (CAS numbers: 106-89-8 (chloromethyl-oxirane) and 3221-15-6 (chloromethyl-thiirane), both having certified purity > 97%) were purchased by Manchester Chemicals Ltd (UK), purified by distillation and stored in dark glass sample tubes.

COMPUTATIONAL DETAILS

Static *ab initio* calculations

The geometry optimizations of each conformer and transition state were accomplished at the B3LYP/6-311++G(3df,3pd) level of theory using Gaussian16 package [7]. Transition states were identified using QST2 method, and, for both energy minima and saddle points, frequencies were checked in order to ensure that the correct stationary point had been found.
The calculations were performed for the molecules *in vacuo* as well as for the molecules placed in a polarizable continuum [8], choosing CCl_4, CS_2, CH_3OH, $(CH_3)_2CO$, DMSO and H_2O as probe solvents. Further calculations were done within the polarizable continuum model (PCM) approximation using the experimental value of the dielectric constant of chloromethyl-oxirane (22.6) [9], whereas the value for chloromethyl-thiirane was estimated from a statistical analysis based on similar molecules where the oxygen atom is replaced by sulphur. This simple procedure would suggest that the approximate ratio between the dielectric constant of molecules containing a closed carbon-sulphur-carbon fragment and the corresponding ones with a closed carbon-oxygen-carbon fragment is about 3/4. According to this observation the dielectric constant of chloromethyl-thiirane was set equal to 17. All the theoretical spectra were computed both in the harmonic and anharmonic approximations at the B3LYP/6-311++G(3df, 3pd) level.
The relative stability of each form was eventually determined by G4MP2 method implemented in the Gaussian package. Population analysis was accomplished on the ground of these calculations using the $\Delta G°_T$ values calculated at appropriate temperatures. These estimates are based on the relation $\Delta G°_T = - RT \ln K_T$ where K_T the thermodynamic equilibrium constant for a given conformational exchange, is the ratio X_j / X_i between the j- pair of conformers.

Ab initio molecular dynamics

To investigate the conformational abundances in the presence of explicit solvent molecules, we considered four different simulation boxes, composed of 1 solute molecule and 10 solvent ones each. The computational protocol adopted is the same of previous works [10-14]. For all the systems, a pre-equilibration was performed with classical molecular dynamics within periodic boundary conditions, using the AMBER [15] program package and the Gaff force field.[16] A 2 ns-long equilibration trajectory was produced for the systems in the NPT ensemble; the simulation temperature was set at 300 K. The final configurations of the classical trajectories were used as starting points for the *ab initio* molecular dynamics simulations, that were accomplished with the program package CP2K,[17] using the Quickstep module.[18] The electronic structure was calculated in the framework of Density Functional Theory using the PBE[19] functional, with the explicit van der Waals terms according to the empirical dispersion correction (D3) by Grimme.[20] The excessive computational cost prevented us from employing, as it was done instead in the static modeling, the more accurate hybrid B3LYP functional. A further simplification was the use of smaller methanol instead of DMSO to model the polar environment, given that these two solvents have both large polarity. Basis sets belonging to MOLOPT-DZVP-SR-GTH[21] family and GTH pseudopotentials[22] were applied; the time step chosen was 0.5 fs and the target temperature

was set at 300 K by a Nosé-Hoover chain thermostat. After 7 ps of QM-equilibration, NVT trajectories of 50 ps were obtained. The neat liquids were also investigated at three selected temperatures, namely 300 K, 200 K and 150 K.

RESULTS AND DISCUSSION

Static *ab initio* calculations

The three stable conformers (*gauche-2*, *gauche-1* and *cis*) of the molecules and the transition states (*TS1*, the transition state between *gauche-2* and *gauche-1, TS2,* between *gauche-1* and *cis,* and *TS3,* between *cis* and *gauche-2)* are represented in **Figure 1**, along with the reaction path connecting them.

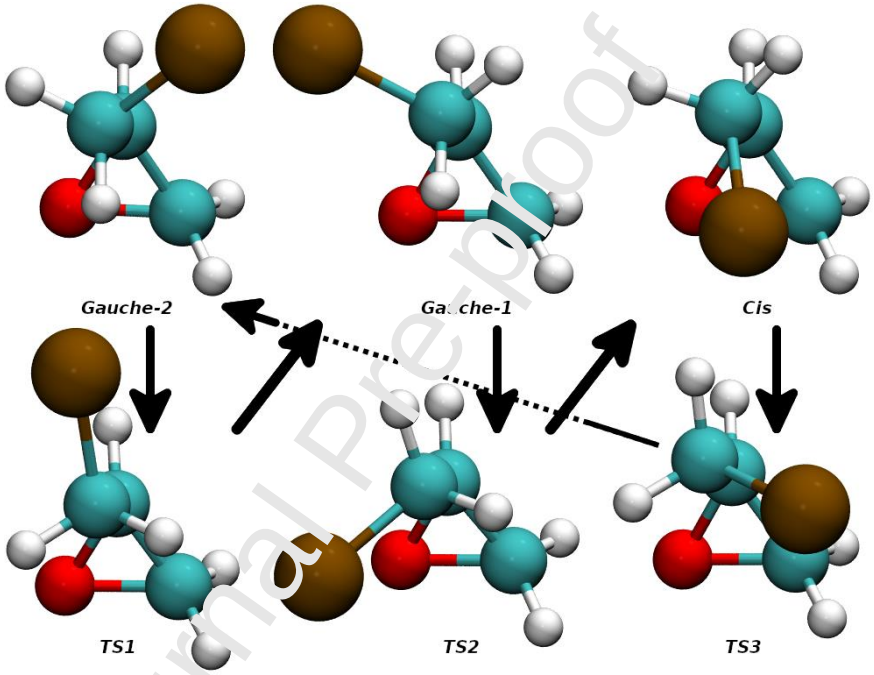

Figure 1 Conformers of chloromethyl-oxirane and chloromethyl-thiirane. The brown atom represents the S or O atom of the two molecules.

The examination of the wide number of calculations carried out for the two *gauche* and the *cis* conformers of chloromethyl-oxirane and chloromethyl-thiirane, as well as for all the transition states between them, led to the following results, which are going to be discussed separately.

(a) Moderate structural effects occur for a given conformer depending whether it is a free species (*in vacuo*) or a species placed in a polarizable continuous medium. Non-polar media were simulated through CCl_4 and CS_2 solvents, while the simulation of polar environment was performed using a series of polar molecules, such as H_2O, DMSO, methanol and acetone. Liquid phase was instead simulated by imposing the polarizable continuum to have the experimental (or estimated) dielectric constant of chloromethyl-oxirane (or chloromethyl-thiirane), as previously described.
In order to examine first the structural effects, the Cl-C-C-O (or Cl-C-C-S) value of the dihedral angle was assumed as a suitable structural parameter useful to distinguish each conformer. With this aim, a useful comparison can be done employing the values found for the gas phase conformers and for the conformers in CCl_4 (non-polar solvent), DMSO (polar solvent)and in “liquid” phase, as reported below:

Table 1: Calculated Cl-C-C-O and Cl-C-C-S dihedral angles (PCM)//B3LYP/6-311++G(3df, 3pd))

	chloromethyl-oxirane				chloromethyl-thiirane			
	in vacuo	**CCl_4**	**liquid**	**DMSO**	***in vacuo***	**CCl_4**	**liquid**	**DMSO**
gauche-1	-82.5	-81.1	-79.1	-78.7	-81.6	-80.5	-79.1	-79.0
gauche-2	162.1	162.1	162.1	162.0	161.8	162.1	162.1	162.3
cis	52.0	51.0	49.3	49.0	49.2	48.9	48.2	48.2

The values reported in **Table 1** indicate that the dihedral angle of *gauche-2* form never undergoes variations for both molecules and that at the same time the variations are quite small for the remaining two conformers across all the calculation models.
Such limited variations are however consistent, producing a decrease in the Cl-C-C-O(S) angle when the polarity of the continuum increases. This decrease nears the two most negatively charged atoms of the molecule (chlorine and oxygen or sulphur), placing them "on the same side" of the structure. The dipole moment of the compound is therefore increased (as can be appreciated in **Tables 1** and **2** of the Supporting Information) and the polar interactions with the solvent maximized.

Table 2 G4MP2 Gibbs free energy differences [cm^{-1}] calculated between the stationary points[(a)] in different solvents.

chloromethyl-oxirane				
	in vacuo	**CCl_4**	**liquid**	**DMSO**
***gauche-2* ↔ *TS1* (to *gauche-1*)**	1303	1300	1277	1273
gauche-1* ↔ *TS1	1108	1200	1377	1393
gauche-2* ↔ *gauche-1	195	100	-100	-120
***gauche-1* ↔ *TS2* (to *cis*)**	1961	1924	1872	1869
***cis* ↔ *TS2* (to *gauche-1*)**	1684	1614	1512	1503
gauche-1* ↔ *cis	278	310	360	365
gauche-2* ↔ *cis	473	409	260	246
***cis* ↔ *TS3* (to *gauche-2*)**	846	912	1045	1057
***gauche-2* ↔ *TS3* (to *cis*)**	1319	1322	1305	1303
chloromethyl-thiirane				
	in vacuo	**CCl_4**	**liquid**	**DMSO**
***gauche-2* ↔ *TS1* (to *gauche-1*)**	1855	1843	1819	1816
***gauche-1* ↔ *TS1* (to *gauche-1*)**	1435	1501	1628	1650
gauche-2* ↔ *gauche-1	420	343	191	166
***gauche-1* ↔ *TS2* (to *cis*)**	2130	2092	2042	2036
***cis* ↔ *TS2* (to *gauche-1*)**	1676	1638	1585	1578
gauche-1* ↔ *cis	455	454	457	458
gauche-2* ↔ *cis	875	797	648	624
***cis* ↔ *TS3* (to *gauche-2*)**	1046	1113	1229	1249
***gauche-2* ↔ *TS3* (to *cis*)**	1920	1910	1878	1872

[(a)] When a transition state is involved, the final arrival point of the reaction is written into parentheses

(b) Energy differences between conformers and transition states have been calculated at G4MP2 level and are reported in **Table 2**. For transition states, the Gibbs free energy has been calculated

by ignoring the contribution coming from the normal mode associated with the conformational conversion, as done automatically by Gaussian package.

There is fully evidence that the energy differences separating the three stable conformers depend on the molecular environment. Concerning chloromethyl-oxirane, for instance, *in vacuo* simulations show that the energy difference between the two *gauche* conformers amounts to around 200 cm^{-1}; such an energy gap decreases in the apolar media (100 cm^{-1}) and eventually changes its sign in the molecular liquid, where *gauche-1* is more stable than *gauche-2*. Energy separations between the two *gauche* conformers and the *cis* one range, in the gas, between 278 and 473 cm^{-1} and have opposite behavior: the *gauche-1*↔*cis* gap increases when the polarity of the surrounding solvent increases while, in the same conditions, the *gauche-2*↔*cis* gap decreases. In chloromethyl-thiirane, instead, the energy difference separating the less stable polar conformer *gauche-1* from the less polar and more stable form *gauche-2* reaches its largest value in gas phase (420 cm^{-1}), decreases in apolar environment (343 cm^{-1}) and it is more or less of the same amount (166 and 191 cm^{-1}) in the liquid and in DMSO, where it is found to reach the lowest values. The calculations predict that the less stable polar conformers of chloromethyl-thiirane always keep their energy separation quite constant around 450 cm^{-1}, therefore testifying that they are stabilized by the interaction with the medium in an equal amount. The high energy gap calculated for the *cis* conformer with respect to the *gauche-2* form (375 cm^{-1} *in vacuo*, 797 cm^{-1} in CCl_4 648 cm^{-1} for the liquid and 624 cm^{-1} for DMSO solvated compound) is determining for its remarkably scarce abundance.

The influence of the solvent on the conformational barriers is another valuable result accomplished from the calculations. Owing to the swinging stability found for chloromethyl-oxirane, where the ordering of the two gauche conformers may change, it is preferable to split the discussion into two parts. When *gauche-2*>*gauche-1* (*in vacuo* and in apolar solvents), the conformational barriers from *gauche-2* to *gauche-1,* from *gauche-1* to *cis* and from *gauche-2* to *cis* substantially remain of the same magnitude (on average 1300, 1950 and 1320 cm^{-1}, respectively), whereas the conversion of *gauche-1* into *gauche-2* and of the less stable conformer *cis* into the most stable *gauche-2* form would depend on the physical surrounding *(in vacuo*: *gauche-1* →*gauche-2,* 1108 cm^{-1} and *cis* → *gauche-2*, 846 cm^{-1}; *gauche-1* →*gauche-2,* 1200cm^{-1} and *cis* → *gauche-2,* 912 cm^{-1} in CCl_4), showing that these conversions are kinetically favored in gas phase.

When the polar form *gauche-1* becomes more stable than *gauche-2*, that is in the liquid and in polar solvents, the conversion between the two *gauche* forms requires an average energy value corresponding to 1300 cm^{-1} while 1050 cm^{-1} would be requested to convert *cis* into *gauche-2* and a larger amount to convert *gauche-1* into *cis*, namely 1870 cm^{-1}.

As could be expected due to the greater steric bulk of sulphur with respect to oxygen, the heights of the conformational barriers of chloromethyl-oxirane are markedly lower than those computed for chloromethyl-thiirane. For this latter compound, the barrier height separating *gauche-1* from *gauche-2* is found to be quite similar both in the liquid and in polar solvents (1640 cm^{-1}), slightly higher than in apolar solvents (1501 cm^{-1}) and in the gas (1435 cm^{-1}). The conversion from *cis* to *gauche-1* is ranging around 1578-1676 cm^{-1}. At last, the conversion between *gauche-2* and *cis* requires around 1900 cm^{-1} in every medium. In general, it can be observed that for this compound the solvent effect on the kinetics is less strong than in the case of chloromethyl-oxirane.

(c) The differences in energies previously described obviously reflect on the conformer abundances, whose values are summarized in **Table 3** for different solvation media. It is also very useful, in order to rationalize the differences in stability among different solvents, to refer to the molecular dipole moment values, which are reported in **Tables 1** and **2** of the Supporting Information.

Table 3 Conformational populations in different solvents[(a)] at 298 K

	chloromethyl-oxirane			chloromethyl-thiirane		
	gauche-1	*gauche-2*	*cis*	*gauche-1*	*gauche-2*	*cis*
in vacuo	25	**68**	7	12	**87**	1
liquid	**56**	34	10	28	**69**	3
CCl_4	34	**58**	8	16	**82**	2
CS_2	36	**56**	8	17	**81**	2
CH_3OH	**55**	35	10	29	**68**	3
$(CH_3)_2CO$	**54**	36	10	29	**68**	3
H_2O	**57**	32	10	30	**67**	3
$(CH_3)_2SO$	**56**	34	10	29	**68**	3

(a) G4MP2 PCM calculations

The most valuable results obtained for chloromethyl-oxirane and summarized in **Table 3** suggest that the *gauche-2* conformer is the most abundant form in the gas phase (*in vacuo* calculations) as well as in apolar media, whereas polar solvents stabilize the *gauche-1* conformer with respect to the remaining *gauche-2* and *cis* forms. It is well known that there exists a relationship between stability and molecular polarity; therefore, for the gas-phase and the molecule in apolar surroundings, the *gauche-2* form having small dipole moment always predominates over the polar *gauche-1* and *cis* conformers, although the abundance of *gauche-2* decreases passing from the *in vacuo* molecule to the molecule solvated by CCl_4 and CS_2. In polar continua, eventually, the polar *gauche-1* conformer predominates, even if not in an overwhelming way.

Contrariwise, in chloromethyl-thiirane the least polar *gauche-2* conformer is always, regardless of the physical surroundings, the energetically favored conformer and consequently the largely predominant one. Sterical hindrance reasons can with high probability be advocated for such a phenomenon: as can be easily appreciated by inspecting the structures depicted in **Figure 1**, the bulky chlorine and sulphur atoms maximize their distance in *gauche-2* conformer. Changes in the solvation medium can only produce a slight population redistribution, without reverting the stability order: in gas phase, the *gauche-2* conformer reaches its maximum (slightly less than 90%), decreases around 80 % in apolar solvents and stabilizes around 70% in the liquid and in polar solvents.

An additional consideration provided by the calculations regards the effect of temperature on the conformational abundances shown in **Table 3** of the Supporting Information. For both the compounds this effect is almost negligible within the temperature range explored and, as could be expected, only a limited shift of the conformational equilibrium towards the less abundant forms can be appreciated.

(d) Frequencies have been calculated using both harmonic and anharmonic approaches. There are actually some differences between the two distinct sets of calculations, as the sequence of the normal modes might show some crossings that may place a given frequency slightly above or below the corresponding harmonic value. The frequencies are reported in detail in **Tables 4** and **5** of the Supporting Information along with intensities and follow at any rate the same order of the harmonic modes adopted by us in the previous studies [1,2] and by Durig [3,4]; the vibrational assignment is consequently based on it.

Since the solvent treatment may cause frequency shifts, the results from PCM calculations in liquid phase, in an apolar solvent (CCl_4) and a polar one (DMSO) are reported along with *in vacuo* values as well. The shifts are of relatively limited amount and the infrared band intensity pattern is scarcely influenced by the environment. As a matter of fact, the comparison among the theoretical

spectra of each conformer calculated in the gas phase and in the different solvents reveals that the relative intensities remain substantially unchanged.

The infrared theoretical spectra are shown in **Figure 2a** and **Figure 2b** in the wavenumber range up to 1400 cm^{-1}, which is the spectral region of major interest. The computed bands are the weighted-sum spectra at 300 K of chloromethyl-oxirane and chloromethyl-thiirane, respectively. making use of populations reported in **Table 3**.

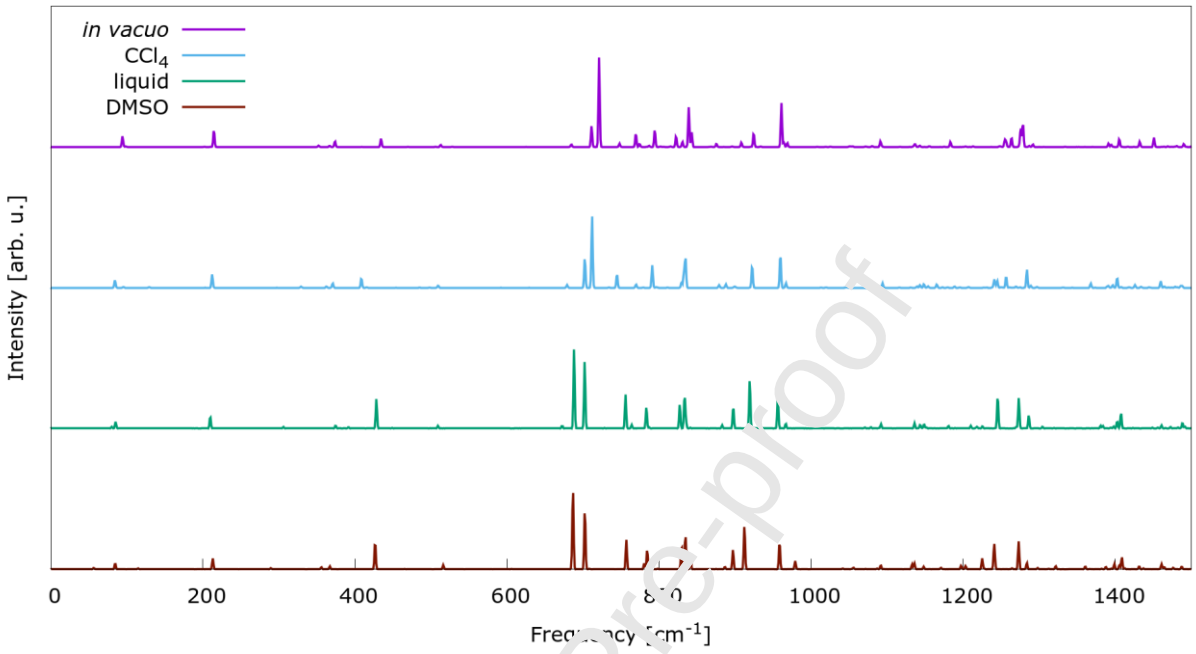

Figure 2a Theoretical IR spectra of chloromethyl-oxirane in different solvents

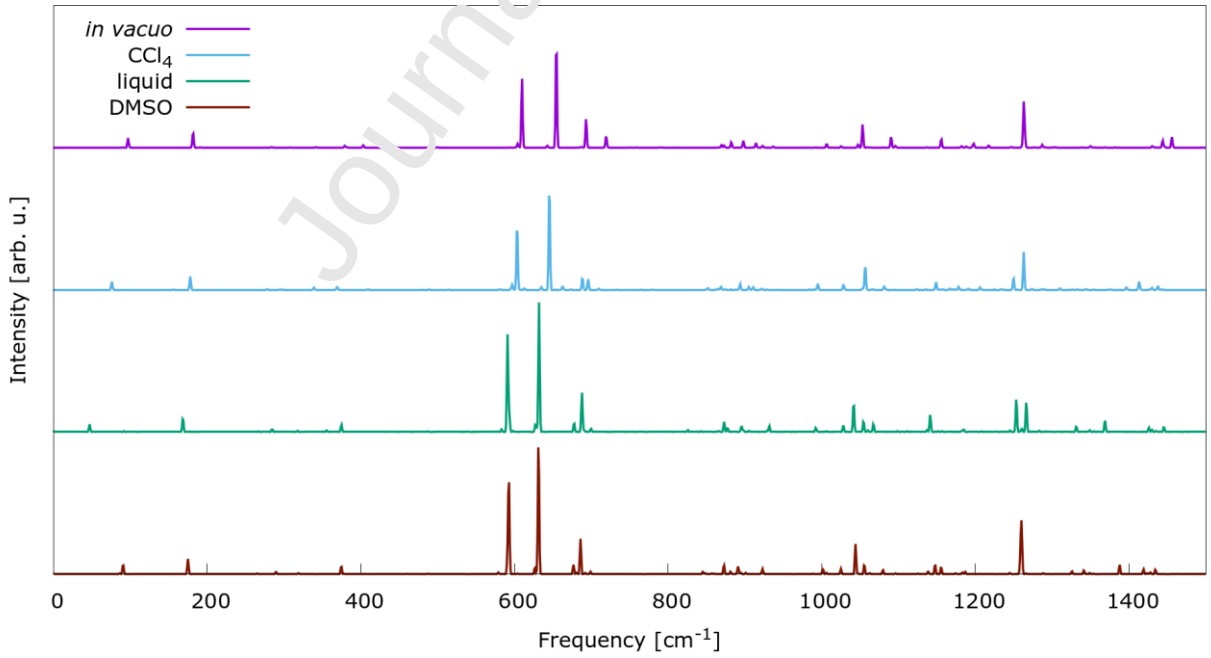

Figure 2b Theoretical IR spectra of chloromethyl-thiirane in different solvents

On the ground of these computational data, it is interesting to spend a few words about the main results accomplished. First, the calculations show a substantial resemblance between the spectrum

of the single molecule and that of the molecule in the apolar surrounding (CCl_4 continuous medium) and this effect is shared by both molecules.
The best representation of the spectrum of the liquid would hopefully be provided by the "liquid" model - PCM calculation with the experimental value of the dielectric constant of chloromethyl-oxirane [10]. With respect to the *in vacuo* calculation, the main difference produced by the PCM approximation can be found around 700 cm^{-1} and 900 cm^{-1}. At last, it is particularly evident the effect of the polar solvent DMSO on the doublet at 700 cm^{-1}.
The computed spectra of chloromethyl-thiirane shown in **Figure 2b** are relatively simple (with respect to chloromethyl-oxirane) since only two conformers significantly contribute to them, being the *cis* conformer abundance actually negligible. For this molecule, PCM spectra appear quite similar among themselves since the predominance of the *gauche-2* conformer is always large with respect to the polar form *gauche-1.*

AIMD simulations

In order to assess if the investigated conformational equilibrium could be predicted with a theoretical method that includes the solvent effects by explicitly considering surrounding molecules, and to further cross-check our analysis, we performed some *ab initio* Born-Oppenheimer molecular dynamics simulations of the liquids. Thanks to this method, it is possible to go beyond both the limits coming out from the force field parameters of classical molecular dynamics and the approximations underlying static PCM approach, obtaining more reliable structural results.[33-35] Due to the limited size of the box currently affordable with AIMD, though, we could not describe the medium-long correlations present in the mixtures, and our exploration was limited to short distances only. The effects of the solvent on the conformers stability and their relative abundances were obtained from the analysis of the C-C-C-Cl Dihedral angle Distribution Functions (DDFs) of the four AIMD simulations trajectories (the plot and its integral are reported in **Figure 3** for chloromethyl-oxirane in methanol and CCl_4) whereas the effect of the temperature was evaluated for the pure liquids only, by monitoring the same dihedral angle distribution.
Regarding chloromethyl-oxirane, it can be seen that both in polar and apolar environment three distinctive conformers are found, with relative percentage values depending on the dielectric constant. In pure chloromethyl-oxirane at 300 K there is moderate prevalence of the polar *gauche-1* form (43%) over *gauche-2* (41%), being the amount of the other polar *cis* type conformer (16%) rather negligible. In chloromethyl-oxirane/methanol the most abundant conformer has a dihedral angle centered at about -167 degrees (weighting 60%), while the other two structures have an equilibrium angle of 68 and 178 degrees respectively, with abundances 22% and 18%. At the same temperature, in the apolar solvent CCl_4 the conformational population changes meaningfully (37% *gauche-1*, 43% *gauche-2* and 20% cis).
In chloromethyl-thiirane, on the contrary, we find only one predominant species (*gauche-2*) in every environment, with only a small effect on the population (64% in neat liquid, 58% in CCl_4, 55% in methanol).
The agreement of these results with those obtained from static PCM calculations is overall satisfactory; the only discrepancies concern a generally overestimated abundance of *cis* conformer in the case of chloromethyl-oxirane and a general underestimate of the most stable *gauche-2* conformer in the case of chloromethyl-thiirane.

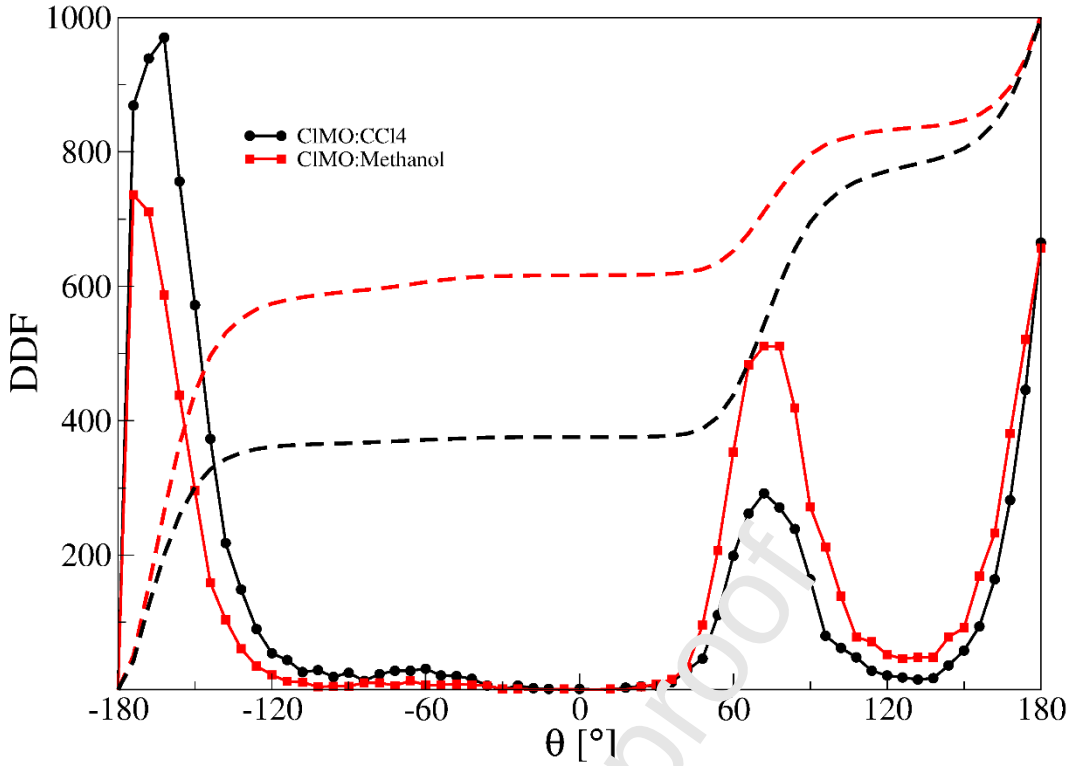

Figure 3 C-C-C-Cl dihedral distribution function of chloromethyl-oxirane in different solvents. Black: CCl4 Red: methanol. Dashed lines: distribution integral.

The effect of temperature was taken into account exclusively for the pure species in the range 150-300 K (see **Table 8** of the Supporting Information). The main conclusion that could be drawn from the calculations is that the *gauche-1* conformer (with the highest dipole moment) is found to increase its amount with respect to the two remaining forms for chloromethyl-oxirane during temperature lowering, as observed in FTIR spectra (see next section). For chloromethyl-thiirane, as temperature decreases the *gauche-1* form converts into *gauche-2* again in line with the experiments. This last issue apparently conflict with the fact that a polar species should be favored in the solid state but, as already discussed, steric effects produced by the large bulkness of sulphur atom most probably come into play, overturning the rough considerations that can be drawn relying on molecular polarity only.

Experimental measures

The large quantity of computational results is someway useful for the interpretation of a series of experimental results. The FTIR spectra were recorded at several temperatures ranging from 300 K down to 160 K and the bands measured in the liquid and solid state of chloromethyl-oxirane and chloromethyl-thiirane are summarized in **Table 4 and 5**. It should be purposely reminded that chloromethyl-oxirane is a liquid compound at ambient temperature and its melting point is 248 K meaning that at 230 K, and obviously below, it is a solid compound. The melting point of chloromethyl-thiirane is 255 K, just 7 K higher than chloromethyl-oxirane. Among the large number of spectra, the FIR and MIR spectra measured at 300 K, 240 K, 200 K and 160 K are shown in **Figures 4a and 4b** for both molecules and all the bands observed are summarized in **Table 4** along with the conclusive assignment of the fundamental modes of each conformer. The spectrum at 240K is shown along with that of the liquid (T=300K) and of the solid (T=160K) samples because this spectrum refers to that of the solid in a state which cannot be considered as crystalline. All the low-temperature spectra below 240 K show no valuable changes during freezing down to 190 K

suggesting that the solid phase between 240 and 190 K is actually an amorphous solid or a supercooled liquid. The spectra recorded at different temperatures below 190 K (namely, 180, 170 and 160 K) appear thoroughly identical among themselves. What meaningfully distinguishes the spectra measured at the three lowest temperatures from the previous ones of the amorphous recorded above 190 K is visualized in **Figures 5a** and **5b**. The band at 963 cm^{-1} disappears below 190 K, the bands at 927 cm^{-1}, 854 cm^{-1}, 759 cm^{-1} appear as doublets at 160 K (928 - 923 cm^{-1}, 854-860 cm^{-1}, 760-755 cm^{-1}) while the peak at 759 cm^{-1} shows a complex band contour consisting of four components lying at 721, 718, 714 and 712 cm^{-1}. More generally, the inspection of all the spectra of chloromethyl-oxirane shows that temperature lowering produces moderate frequency shifts, as well as expected infrared band intensity modifications, with regard to the spectrum of the liquid collected at 300 K. A further note to be added concerns the behavior of some bands lying between 1355 and 1330 cm^{-1}, as well as those between 1200 and 1000 cm^{-1}, which start to take

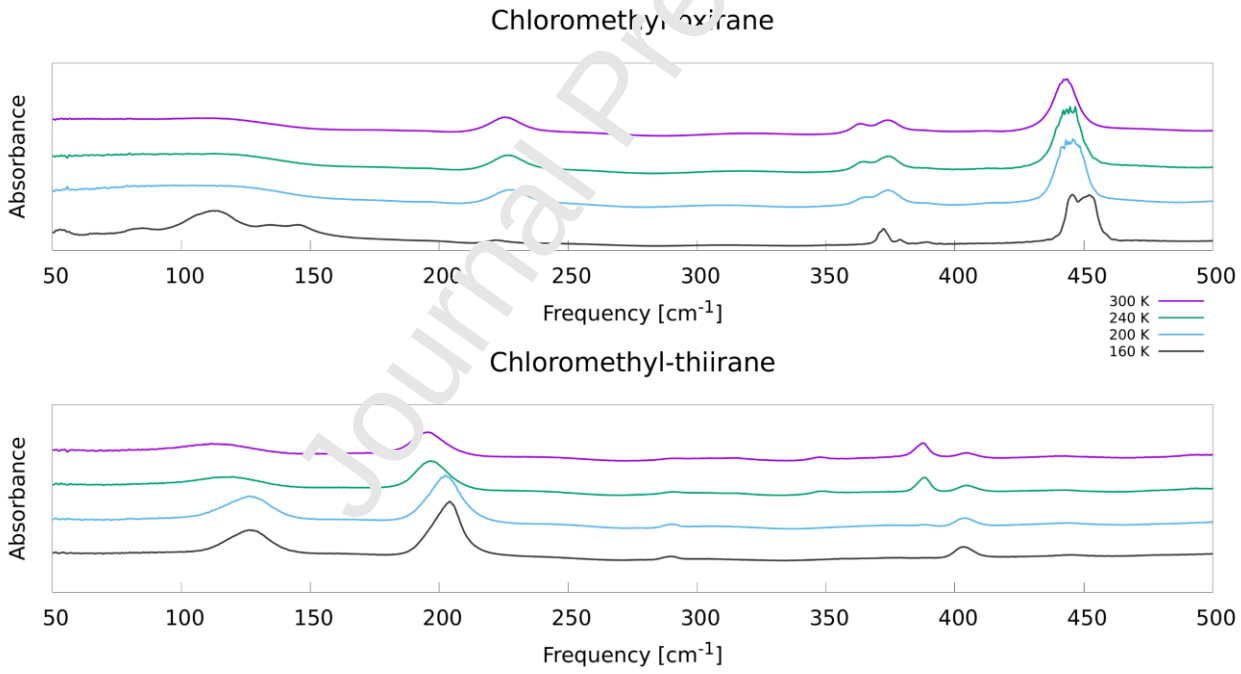

Figure 4a FIR spectra measured at four significant temperatures (160, 200, 240 and 300 K).

shape when the solid sample temperature is lowered from 240 K; all these bands become more definite and appear quite neat at 160 K.

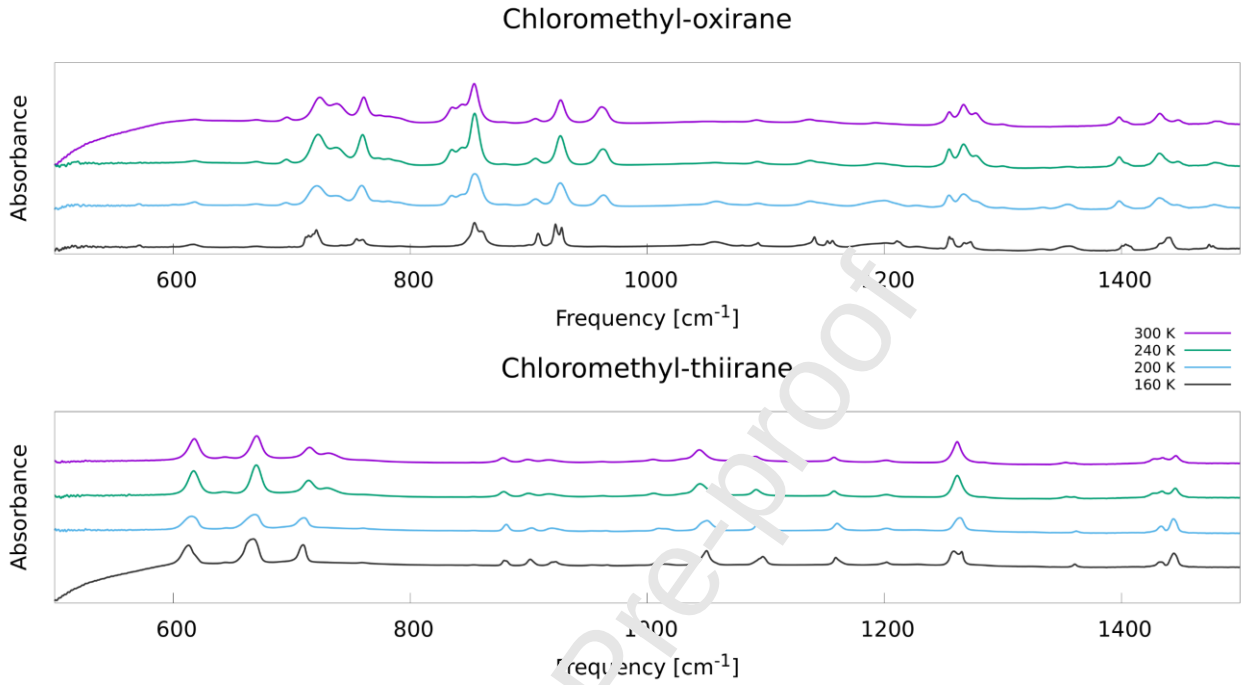

Figure 4b MIR spectra measured at four significant temperatures (160, 200, 240, 300 K).

band assignment

Table 4 Measured FTIR spectra (cm-1) of chloromethyl-oxirane and chloromethyl-thiirane

		Chloromethyl-oxirane			Chloromethyl-thiirane			
Mode	**Gas**	**Liquid (300K)**	**Solid (240K)**	**Solid (190K)**	**Gas**	**Liquid (300K)**	**Solid (240K)**	**Solid (190K)**
υ1gauche-2	**3063**				**3081**	**~ 3072**	**~ 3072**	**3069**
υ1gauche-1	3056	3062	3065	3068-3072	3074	(g)3062		
υ1cis	3068							~ 3030
υ2gauche-2	(b)3024				3036	~ 3021	~ 3020	3021
υ2gauche-1		(d) 3022		~3030 3017	(f) 3018	(g) 3009		
υ3gauche-2	(b) 3008				3008	(g) 3010		3008
υ3gauche-1	(b)3015	3004	3004	3007	(f) 3024	~ 3018		
υ3cis	(c) 2991							
υ4gauche-2	2975				(f) 2995	2991	2990	2989
υ4gauche-1	2963	2963	2964	2969-2973	(f) 2954	(g) 2976		

υ5 gauche-2	(b) 2942				2976	2962	2961	2963
υ5 gauche-1	2936 (b)	2925	2925	2924-2927	(f) 2940	2944	2943	
						~ 2891		
						2861	~ 2859	2858
						~ 2837		
υ6gauche-2	1490	1483		1488	1456	1446	1445	1444
υ6gauche-1	1487	1480	1479	1474	1447	1446	1434	
				-1477				
υ7gauche-2	1456				1435	1435	1434	1433
υ7gauche-1	1437	1432	1432	1439-1441	(f) 1429	1428		
υ7cis	1439	1448	1447					
υ8gauche-2	1412				1363	~1360	1362	1361
υ8gauche-1	1405	~1404		1408-	1350	1353		
				14061404-				
				1401				
υ8cis	1402	1398	1398					
			1354	~1356				
				~1333				
						~ 1284		
υ9 gauche-2	1276	1277	~1278		1264	1261	1264	1265-1259
υ9 gauche-1	1267	1267	1267	1267-1273	(f) 1256	1261		
υ9 cis	(c) 1292	1299	~1300					
υ10 gauche-2	1246				1196		1202	1202
						{1202}*		
υ10 gauche-1	1253	1255	1255	1255-1257	1202			
υ10 cis	1256							
				1227				
υ11 gauche-2	1194	1192	1200		1159	1157	1158	1159
υ11 gauche-1	(c) 1207	~ 1208		1211-1213	(f) 1157	(g) 1141		
υ11 cis	(c) 1202	(d) 1197	1196					
υ12 gauche-2	1136							
					{1091}*	{1091}*	{1092}*	{1097}*
	1151	~1147	~1149	1152-1156				
υ12 gauche-1								
υ13 gauche-2				{1141}*	1043	(g) 1050		1050
υ13 gauche-1	{1134}*	{1137}*	{1138}*					
υ13 cis								
υ13 gauche-1					1040	1044	1044	
								~ 1017
υ14 gauche-2					1007	1005	1005	1007
υ14 gauche-1	{1092}*	{1092} *	{1092} *	{1094} *				
					(f) 1028	~1029		
				1080				
υ14 cis	1073	~1072						
								966
						962	962	953
υ15 gauche-2	(c) 1053				923	917	917	923-920
υ15 gauche-1	(c) 1057	(d) 1055	1058	1057	(f) 937			

				1039				
υ15 cis	(c) 1034	~1031						
υ16 gauche-2	964	961	963		898	899	900	901
υ16 gauche-1	934	927	927	928-923	883	(g) 880		
υ16 cis	972	961	963					
υ17 gauche-2	(c) 875	879	880		879	878	879	879
υ17 gauche-1	(c) 911	906	906	908	915	(g) 913		
				900				
			881			~853		
						~762		
υ18 gauche-2	842	844	844		731	715	714	710
υ18 gauche-1	853	854	854	854-861	751	731	730	
υ18 cis	838 (c)	836	835-843					
υ19 gauche-2	794	~791	~790		686	670	670	667
		~783	782					
υ19 gauche-1	775	760	759	755-760	(f) 65[illegible]	644	642	
υ19 cis	~788	~774	~773					
υ20 gauche-2	756	738	737		[illegible]27	618	617	613
υ20 gauche-1	743	724	721	721-718	6[illegible]2	618	617	
				714-712				
υ20 cis	(c) 703	696	695	698-[illegible]				
		671	670	671				
		618	618	61[illegible]				
υ21 gauche-2	(c) 405	~412			402	405	404	404
υ21 gauche-1	438	443-442	446	445-452	388	387	388	
υ21 cis	521	518	519					
				389				
				379				
υ22 gauche-2					278	291	291	290
υ22 gauche-1	{(b)	{363-	{36[illegible]-	{373}*				
	371}*	374}*	374}*		351	348		
υ23 gauche-2	(b) 214	225	227		189			
								204
υ23 gauche-1		225	227	222		195	197	
υ24 gauche-2	~ 90				99		119	126

(a) IR, gas, Ref. [1]
(b) Raman, gas, Refs. [1]
(c) IR, Xe matrix, Ref. [1]
(d) Raman, liquid, Ref. [1]
(e) IR, gas, Ref. [2]
(f) IR, Xe, Ref. [2]
(g) Raman, liquid Ref. [2]

* bands reported in curly brackets belong to both *gauche conformers*

Table 5 low temperature bands (cm^{-1}) of chloromethyl-oxirane and chloromethyl-thiirane

	Chloromethyl-oxirane[(a)]								
T/K→	**240**	**230**	**220**	**210**	**200**	**190**	**180**	**170**	**160**
U_1gauche-1	3065	3065	3065	3065	3064	3065	3068	3068	3068 3072
							3017	3018	3017
U_3 gauche-1	3004	3004	3004	3004	3004	3004	3004	3004	3007
U_4 gauche-1	2964	2963	2963	2963	2963	2963	2969	2969	2969 2973
U_5 gauche-1	2965	2925	2925	2925	2925	2925	2927	2927	2924 2927
							2878*	2879	2879
									2862*
U_6 gauche-2							1488*	1488*	1488*
U_6 gauche-1	1479	1479	1479	1478	1478	1478	1477 1474	1477 1474	1477 1474
U_7 gauche-1						1437	1441 1439	1441 1438	1441 1438
U_7 cis	1447	1447	1447	1447	1447	1449 1446			
U_7 gauche-1	1432	1432	1432	1432	1432	1432	1432	1432	1433
U_8 gauche-2								1407	1408 1406
U_8gauche-1	1398	1398	1398	1398	1398	1398	1404 1401	1404 1401	1404 1401
	1356 *	1356 *	1356 *	1354	1354	1354	1356	1356	1356
			1334 *	1334 *	1334	1334	1333	1333	1333
U_9 cis	1300	1300	1300 *	1300*	1301	1301			
U_9gauche2	1278	1278	1277	1278	1279	1281			
U_9 gauche-1	1267	1267	1267	1267	1267	1267	1267 1273	1267 1273	1267 1273
U_{10} gauche-1	1255	1255	1255	1255	1255	1255	1255 1257	1255 1257	1255 1257
U_{10}gauche-2								1248*	1248*
				1227*	1227	1227	1227*	1227*	1227*
U_{11} gauche-1							1211	1211	1211 1213
U_{11}cis	1194	1195	1196	1199	1200	1200	1200*	1201*	1201*
U_{12} gauche-1							1156 1152	1156 1152	1156 1152
U_{12} gauche-2	1137	1138	1138	1138	1137	1138	1141	1141	1141
U_{14} gauche-2	1093	1093	1093	1093	1093	1093	1093	1093	1094
							1080*	1080	1080
								1038	1039
U_{15} gauche-1	1057	1057	1058	1058	1058	1058	1057	1057	1057
U_{16} cis	961	961	961	961					

U_{16} *gauche-1*	927	927	927	927	927	927	928	928	928
							923	923	923
U_{17} *gauche-1*	906	906	906	906	906	906	908	908	908
							900*	900*	900*
U_{17} *gauche-2*	881*	881*	880*	880*	881*	880*			
							860	860	
U_{18} *gauche-1*	854	854	854	854	854	854	854	854	
U_{18} *gauche-2*	845	844	844	844	844	848			
U_{18} *cis*	835	835	835	835	835	835			
								818*	
U_{19} *gauche-2*			791*	791*	791*	790*	791*	791*	791*
			781*						
			773*						
U_{19} *gauche-1*	760	760	759	759	759	759	760	760	
							756	**755**	
U_{20} *gauche-2*	737	737	737	737	737	739	742*	742*	
U_{20} *gauche-1*	722	722	722	722	721	721	721	721	721
							718	718	718
							715	714	714
							712	712	712
									702*
U_{20} *cis*	696	695	695	695	695	695		698*	698*
	670	669	670	670*	670	670*	671		670
							651*		651
	618	617	617	618	617	618	616	616	616
				571*	572*	571*	571*		
U_{21} *cis*	518	518	519	519	519	519			
U_{21} *gauche-1*	445	445	445	446	445	446	451	453	452
							446	445	445
U_{21} *gauche-2*					416*	416*			
	388**	388*	389*	390*	390*	390	389	389	389
U_{22} *gauche-2*	374	374	374	374	374	374	378	379	379
	365	364	365	366	365	366	372	372	372
	318*	316*	316*	316*	311*	307*	314*		
U_{23} *gauche-2*									
	227	227	227	227	227	228	222	222	222
U_{23} *gauche-1*									
							145	144	145
							133	134	134
	119	115				119	112	111	113
U_{24} *gauche-2*							86	84	85
					chloromethyl-thiirane[(b)]				
T/K→	**240**	**230**	**220**	**210**	**200**	**190**	**180**	**170**	**160**
U_1 *gauche-2*	3072	3072	3069	3069	3070	3070	3069	3069	3069

						3031	3032	3031	3032
U_2 *gauche-2*	3023	3022	3023	3023	3018	3021	3021	3021	3021
U_3 *gauche-2*					3004	3008	3008	3008	3008
U_4 *gauche-2*	2990	2990	2990	2990	2989	2989	2989	2989	2989
U_5 *gauche-2*	2961	2961	2961	2961	2960	2963	2963	2963	2963
U_5 *gauche-1*	2943	2944	2943	2944					
		2859	2859	2859	2858	2858	2858	2858	2858
U_6 *gauche-2*	1445	1445	1445	1445	1444	1444	1444	1444	1444
U_7 *gauche-2*	1434	1434	1434	1434	1434	1433	1433	1433	1433
U_7 *gauche-1*	1427	1428	1428	1428					
U_8 *gauche-2*	1360	1360	1360	1360	1362	1361	1361	1361	1361
U_8 *gauche-1*	1354	1354	1354	1354					
	1284	1284	1284	1284					
U_9 *gauche-2*					1264	1265 1259	1265 1259	1265 1259	1265 1259
U_9 *gauche-1*	1261	1262	1262	1262	1264				
					1224*	1228*	1229	1228	1228
U_{10} *gauche-2*					1202	1202	1202	1202	1202
U_{10} *gauche-1*	1202	1202	1202	1202	1202				
U_{11} *gauche-2*	1158	1158	1158	1158	1160	1159	1159	1159	1159
U_{12} *gauche-2*					1097	1097	1097	1097	1097
U_{12} *gauche-1*	1092	1092	1092	1092					
U_{13} *gauche-2*					1050	1050	1050	1050	1050
U_{13} *gauche-1*	1044	1045	1045	1045					
					1017	1017	1018	1018	1018
U_{14} *gauche-2*	1005	1006	1006	1006	1010	1008	1008	1008	1008
					990*				
	962	962	962	963*	965	966	966	966	966
					953*	953*	953	953	953
U_{15} *gauche-2*					920	922 919	922 919	923 919	923 920
U_{17} *gauche-1*	917	917	917	917					
U_{16} *gauche-2*	900	900	900	900	903	901	901	901	901
U_{17} *gauche-2*	879	879	879	879	881	880	880	880	881
U_{18} *gauche-1*									879
	853*	854*	853*	853*	853*	853*	854*	853*	853*
	763	763	763		760*	760*	759*	759	759
U_{18} *gauche-1*	730	730	729	729					
U_{18} *gauche-2*	714	714	714	714	710	710	710	710	710
U_{19} *gauche-2*	670	670	670	670	669	668	667	667	667
U_{19} *gauche-1*	642*	642*	642*	642*	645*				
U_{20} *gauche-2*	617	618	617	617	616	613	613	613	613
U_{20} *gauche-1*	617	618	617	617	616				
	494*	494*	494*	494*					
	442*	443*	443*	442*	445	443*	445		
U_{21} *gauche-2*	404	405	405	405	404	404	404*	403	403
U_{21} *gauche-1*	388	388	388	388	388	389*			
U_{22} *gauche-1*	348	349	349	349					

					304*				
U_{22} *gauche-2*	291	291	291	291	290	290	290	290	290
U_{23} *gauche-2*	197	197	197	198	202	202	203	204	204
U_{23} *gauche-1*	197	197	197	198					
U_{24} *gauche-2*	120	120	120	122	127	127	127	126	126

[(a)] T_{mp} = 255 K
[(a)] T_{mp} = 248 K
* weak or very weak and broad bands

The dependence of the measured spectrum on temperature is of great interest for the purpose of this work. As a general consideration, there are no valuable changes from the spectrum recorded at 300 K and that at 240 K, just below the melting temperature of these liquids. Changes start to be observed during further freezing down to 200 K and just below that temperature the spectra begin to reveal remarkable modifications. The low temperature spectra between 240 K and 200 K could be attributed to amorphous solids (glass, as reported elsewhere [1] for chloromethyl-oxirane) and only below 200 K to a more complex solid state that would reveal bands attributable to crystal along with bands of the amorphous or even to a polycrystalline solid. The reader can follow the spectral modifications due to temperature from the data summarized in **Table 5**. For sake of conciseness, we shall examine and compare the spectra recorded at 300 K, 200 K and 160 K for both molecules.

Chloromethyl-oxirane

Concerning chloromethyl-oxirane, there are some typical bands of the molecule deserving some detailed comment as their vibrational pattern is particularly dependent on temperature.
The three regions of the spectrum showing the major changes are those within 1450-1300 cm^{-1}, 1250–1100 cm^{-1} and in particular between 950-700 cm^{-1}. The spectra below 240 K are relatively sim4ilar to the spectrum measured for the molecule in its liquid phase and one may confidently define this physical state as that of a glassy solid system (amorphous solid). This condensed state endures up to 200 K and is characterized by the coexistence of all the three conformers. The position of the observed peaks does not meaningfully differ from that of the liquid state. Just moderate variations of band intensity are taking place. The intensity of the band at 1432 cm^{-1} (ν_7 *gauche-1*) of the liquid and amorphous gradually decreases its intensity with temperature lowering and at 160 K appears the intense doublet 1443-1433 cm^{-1}. The higher frequency side of the 1432 cm^{-1} band at 1447 / 1448 cm^{-1} (ν_7 *cis*) undergoes the same intensity trend and is no longer observable at 160 K. The relatively medium intensity band around 1480 cm^{-1} is actually a doublet at 300 K with components at 1479-1483 cm^{-1} attributable to the ν_6 mod, that are visible in all the spectra recorded up to 200 K, though slightly shifted to lower wavenumbers, and thoroughly disappear at temperatures below 200 K. A more careful investigation of this band actually would reveal another low intensity component lying in the higher wavenumbers side of the doublet. This very low intensity component assumes the feature of a band at 1488 cm^{-1} only at 160 K. At this temperature, as well as at 190 K and 180 K, two net bands at 1477 and 1474 cm^{-1} appear in the low temperature spectrum in lieu of the broad doublet around 1480 cm^{-1}. One has anyway to mention that a not completely well defined shoulder at 1480 cm^{-1} having low intensity contributes to the profile of the band at 1477 cm^{-1}. The weak intensity band at 1488 cm^{-1} is very likely the band reported by Durig [1] at 1490 cm^{-1} and assigned to the ν_6 *gauche-2* mode in the crystal. Concerning the bands of the doublet 1480-1483 cm^{-1} one cannot exclude that both are due to the ν_6 mode of

both the gauche forms, namely 1480 cm^{-1} (ν_6 *gauche-1*) and 1483 cm^{-1} (ν_6 *gauche-2*).
The ν_8 mode of the liquid is represented by 1404 cm^{-1} (*gauche-1*) and 1398 cm^{-1} (*cis*), being the higher frequency component not particularly well resolved. This pattern undergoes changes starting from 240 K when the whole vibrational structure shifts at higher wavenumbers and eventually produces four sharp bands at 1401, 1404, 1406 and 1408 cm^{-1} at 160 K. The component at 1401 cm^{-1} should correspond to the band measured by Durig at 1399 cm^{-1} (*gauche-1*) for the amorphous and that at 1406 cm^{-1} to that reported for the crystal at 1405 cm^{-1} (*gauche-1)*[1]. The origin of the remaining bands cannot be easily assessed and likely it might be due to solid state effect or alternatively to a complex polymorphic solid state.
The bands of the ν_9 mode characterized by the tidy components at 1277 cm^{-1} (*gauche-2*), 1267 cm^{-1} (*gauche-1*) and 1299 cm^{-1} (*cis*) and the band of the ν_{10} mode of *gauche-1* at 1255 cm^{-1} show large modifications at the lowest temperatures when the three bands are replaced by the low intensity pattern of four bands (1273, 1267, 1257, 1255 cm^{-1}) and a less resolved component (*ca*. 1270 cm^{-1}) and a very weak but resolved band at 1248 cm^{-1}, which might tentatively be assigned to the ν_{10} vibration of *gauche-2*, probably in the crystal.
The spectral region 1200-1050 cm^{-1} displays a series of relatively broad bands found to increase intensity during temperature lowering, although at different extent. At 300 K, from the flatness of this region one may distinguish two wide bands at 1192 and 1137 cm^{-1}; these bands would reveal after a careful sight less intense and wide absorptions at *ca*. 1210, 1156 and 1147 cm^{-1}. During sample cooling these bands retain their profile although it is quite clear that their intensity is increasing. At the same time, step by step, a band at *ca*. 1227 cm^{-1} takes shape, although its intensity is never particularly high. Similarly, other three absorptions occurring at *ca*. 1038, 1060, 1080 and 1000 cm^{-1} display the same trend just reported above. Furthermore, the band around 1060 cm^{-1} badly starts to be revealed at 210 K and quickly reaches fair intensity. This is the scenery up to 190 K; below this temperature, the spectral features show significant adjustments particularly evident around 1150 cm^{-1}. Actually, at 160 K the triplet 1156, 1152 and 1141 $cm^{-1}$is present instead of the band 1137 cm^{-1} observed at higher temperatures. The band measured in the liquid at 1147 cm^{-1} and at 1149 cm^{-1} in the amorphous is assigned to the v12 vibration of gauche-1, while the high intensity peak 1141 cm^{-1} observable in the crystalline phase can be ascribed to the ν_{13} mode of the three species. The origin of the low intensity broad band 1227 cm^{-1} is unknown and likely it cannot be related to any fundamental vibration of the molecule. The two bands at 1080 cm^{-1} (extremely weak intensity) and 1094 cm^{-1} (medium/medium-weak intensity) measured at 160 K could be assigned to the ν_{14} modes of the *cis* and to both the *gauche* conformers, respectively. At last, the remaining bands of the mid-infrared range, which are going to be discussed later, are those showing the largest variations with temperature and play an interesting role in this work. In this wavenumber range, there are no remarkable differences between the spectra of the liquid and those of the glassy state. It is just below 190 K that the spectra point out modifications consisting of the disappearance of the band 960 cm^{-1}, which certainly is one of the expected ν_{16} modes of the molecule and the other band due to the same vibration is measured at *ca.* 930 cm^{-1}. Concerning the assignment of ν_{16}, Durig states that "*it has been found to not be a single band from one conformer but has a line from the cis conformer underneath*" [1]. Our calculations provide for this vibration the results summarized in the following **Table 6** where the anharmonic frequencies (cm^{-1}) and related infrared band intensities (km/mol) are reported:

Table 6 Anharmonic bands (cm^{-1}) calculated for chloromethyl-oxirane

System	*gauche-2*	*gauche-1*	*cis*
Isolated molecule	961 (28)	924 (25)	964 (28)
Liquid	956 (38)	919 (37)	967 (36)

These results suggest that the ν_{16} mode of both the *cis* and *gauche-2* forms occurs at very close wavenumbers; that is actually true for *in vacuo* calculations, whereas the polarizable continuum simulation estimates for the *cis* and *gauche-2* conformer a difference of 11 cm^{-1}. One has to further consider that the intensity ratio of the bands associated with the ν_{16} vibration of *cis* 967 cm^{-1} (0.95) and *gauche-2,* 956 cm^{-1} (1.0) is identical within the limits of the computational procedure. On this basis, it is therefore plausible the overlap of the ν_{16} modes of *cis* and *gauche-2* in the liquid. The observation that the intensity of the band measured at *ca.* 960 cm^{-1} decreases when temperature is lowered would be consistent with the conclusion that the most polar forms (*gauche-1,* with the highest dipole moment and even *cis* the other most polar one) are favorite in the liquid phases, albeit the *cis* conformer is manifestly lacking (or present in extremely scarce amount) in the crystal but still present in the amorphous. From the computational point of view, the PCM estimate of the conformational population at 298 K performed at the G4MP2 level employing the experimental value of the dielectric constant of the molecule [10] produces the interesting result that *gauche-1* is the most stable conformer (58%), followed by *gauche-2* (36%) and *cis* (6%).

It is just below 190 K that the spectra show evident modifications consisting in the disappearance of the band at 961 cm^{-1} (ν_{16} *cis*), at 844 and 836 cm^{-1} (ν_{18} *gauche-2* and ν_{18} *cis*) associated however with the appearance of the intense band at 860 cm^{-1}, likely the ν_{18} *gauche-1* in the crystal. At the same fashion, the region within the range 800–700 cm^{-1} undergoes worthy modifications due to temperature lowering. At 300 K, the liquid shows intense bands at 761 cm^{-1} (ν_{19} *gauche-1*), 738 cm^{-1} (ν_{20} *gauche-2*) and 724 cm^{-1} (ν_{20} *gauche-1*) flanked by the weak band 774 cm^{-1} and the weak, broad and hardly shaped bands 783 and 792 cm^{-1}. These three weak bands deserve some considerations. First, the presence of the band at 774 cm^{-1}, not reported by Durig [1] in the IR spectrum of the liquid, could correspond to the Raman band of the liquid at 773 cm^{-1} and therefore it is assigned to the ν_{19} mode of the *cis* form. The unresolved broad bands measured by us at 783 and 792 cm^{-1} might be related to the same vibration of *gauche-2*. The band 781 cm^{-1} appears more shaped at 200 K while the 792 cm^{-1}, which does not undergo any modification at the same temperature, assumes the typical very weak symmetrical band contour at 160 K. At the lowest temperature of our measurements both bands observed at 781 and 773 cm^{-1} disappear.

As already stated, apart from the frequency shifts characterizing the spectra at 300 K and those below the freezing point up to 200 K, the spectra measured between 240 K and 200 K are quite similar. However, below 180 K, there is clear evidence of huge changes in the range 760- 600 cm^{-1}, being the most remarkable ones those occurring for the intense bands of the spectrum. The band 761 cm^{-1} appears at 160 K as two absorptions having the same intensity at 760 and 755 cm^{-1}, the band around 740 cm^{-1} (ν_{20} *gauche-2)* is completely lacking and the other intense bands around 720 cm^{-1} (ν_{20} *gauche-1)* is replaced by intense absorptions at 721, 718, 714 and 712 cm^{-1}; this observation reveals the complexity of the solid state at 160 K. The spectrum of the glass reports only a very strong peak at 715 cm^{-1} (ν_{20} *gauche-1),* whereas the spectrum of the crystal [1] reports two bands, one at 718 cm^{-1} and another one at 713 cm^{-1}. Excluding ^{37}Cl isotopic effect from the intensity ratios of the four bands present in our spectrum at 160 K, the comparison between our results and those already published [1] would suggest that the strong components of the spectrum measured at 714 and 712 cm^{-1} could be related to the bands reported in literature at 715 cm^{-1} for the amorphous and 713 cm^{-1} for the crystal [1] while the remaining two bands of the solid observed by us at 721 and 718 cm^{-1} might be due to solid state effects.

Evidently, the same considerations reached from the inspection of the mid-IR spectra (namely, similarity between the spectra of the liquid and of the low temperature solid at least up to 200 K) hold for the far IR. The most evident trait of the lowest temperature spectra is the lack in the very low temperature spectrum of the peak at 519 cm^{-1}, the typical vibration of the *cis* form. The *cis*

conformer ceases to exist below 190 K. Further variations can be revealed from the doubling of the high intensity band at 450 cm^{-1} (ν_{21} *gauche-1*), from the reorganization of the band at 365-374 cm^{-1} into two net components at 372 and 379 cm^{-1} (ν_{22} *gauche-1*) and the strong intensity lowering of the bans at *ca*. 220 cm^{-1} (ν_{23} *gauche-1* and *gauche-2*).

Chloromethyl-thiirane

First of all, the mid-IR spectrum appears simpler than that of the former molecular system for the verified lacking in the *cis* conformer, which is indeed below the limit of the experimental detection. The most striking trait is once again the unquestionable similarity between the spectrum of the liquid and the whole series of spectra recorded at decreasing temperatures down to 200 K. This observation implies that both the *gauche* conformers coexist in the amorphous solid. What really marks the higher temperature spectra from those below 200 K is the disappearance of the bands of the polar *gauche-1* conformer and for this reason *gauche-2* is the unique conformer present in the solid in the lowest temperature range of the investigation. In more detail, moving towards higher wavenumbers, one may observe the restyling of the triplet spanning from 1460 to 1420 cm^{-1} associated with the disappearance at low temperature of the lowest wavenumber component 1428 cm^{-1} and with intensity modifications particularly remarkable for the band at 1446 cm^{-1}, that strongly gains its intensity. Another restyling occurs in the range of the ν_8 mode at 1370 and 1340 cm^{-1}. At 300 K, the infrared pattern shows a band at 1353 cm^{-1} and another of minor intensity at 1360 cm^{-1} from which two concealed absorptions at *ca*. 1362 and at 1364 cm^{-1} are barely distinguishable. At 200 K only the band at 1362 cm^{-1} survives while starting from 190 K there is a single and symmetrical band at 1361 cm^{-1} having valuable intensity. The high intensity peak at 1260 cm^{-1}, which retains its sharpness up to 200 K, appears at the lowest temperatures as two distinguishable bands at 1259 and 1265 cm^{-1} (ν_9 *gauche-2*) with the same intensity. The region within the range 500-800 cm^{-1} is also involved in remarkable resettlement, displaying in frequency shifts and band intensities. At 300 K, the bands observed in this range are 731, 715, 670, 644 and 618 cm^{-1}; neglecting the small frequency shifts of these bands, confined within a few wavenumbers, some variations are found in the band intensities associated with these bands when temperature is gradually lowered up to 210 K when the bands, except that at *ca*. 730 cm^{-1}, mildly increase intensity. At 200 K, all these bands appear quite less intense and there is no longer any signal at 730 cm^{-1} (ν_{18} *gauche-1*). From this result one could conclude that below 210 K the *gauche-1* conformer ceases to exist.

The far infrared spectrum does not reveal significant changes from 300 K down to 210 K; in this temperature range the six bands of the spectrum are approximately measured at 404, 388, 348, 291, 197 and 120 cm^{-1}. Among these bands, those observed at 404, 291, and 120 cm^{-1} are assigned to the *gauche-2* form, those at 388 and 348 cm^{-1} to *gauche-1* and the band at 197 cm^{-1} to both the *gauche* conformers. This pattern is basically unchanged from 300 K to 210 K, however starting from 200 K there is no longer evidence of the peak at 388 cm^{-1} and of other bands assigned to *gauche-1.* Without any exception, all the bands due to *gauche-2* are found to increase intensity during the cooling down. There is no doubt that this is a further grounded proof that the solid state consists of *gauche-2* conformers only.

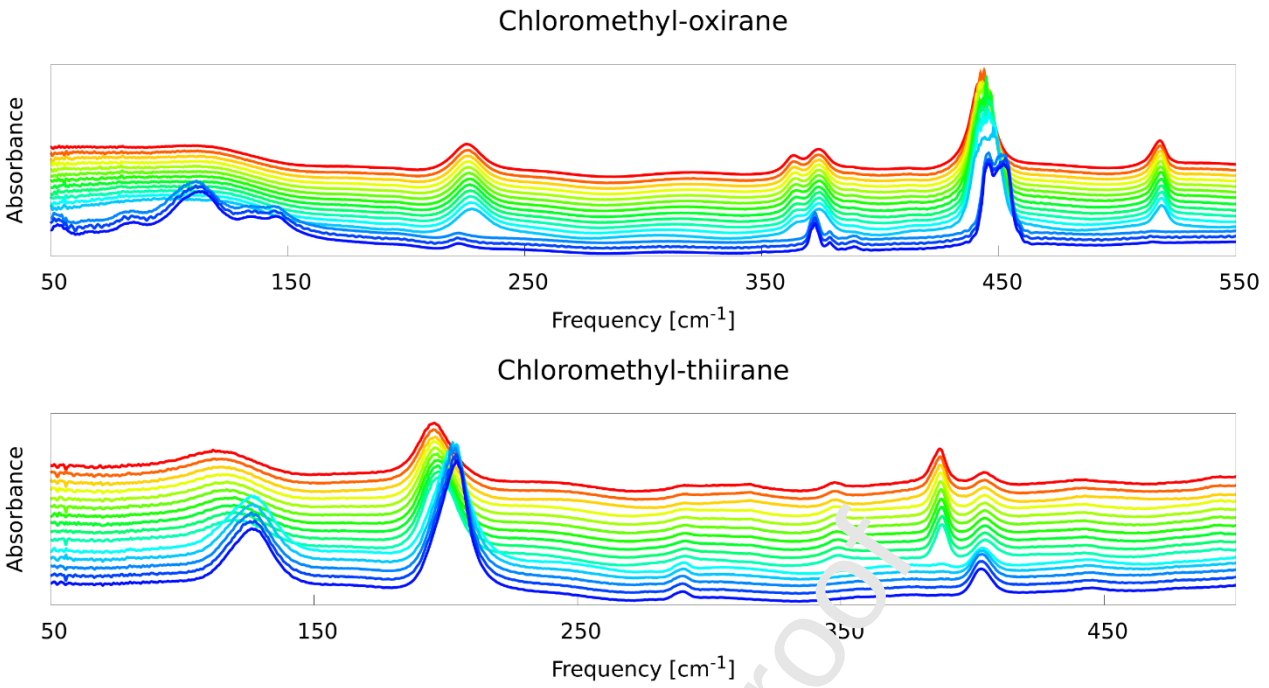

Figure 5a FIR spectra at variable temperature (blue T_{min}, red T_{max}).

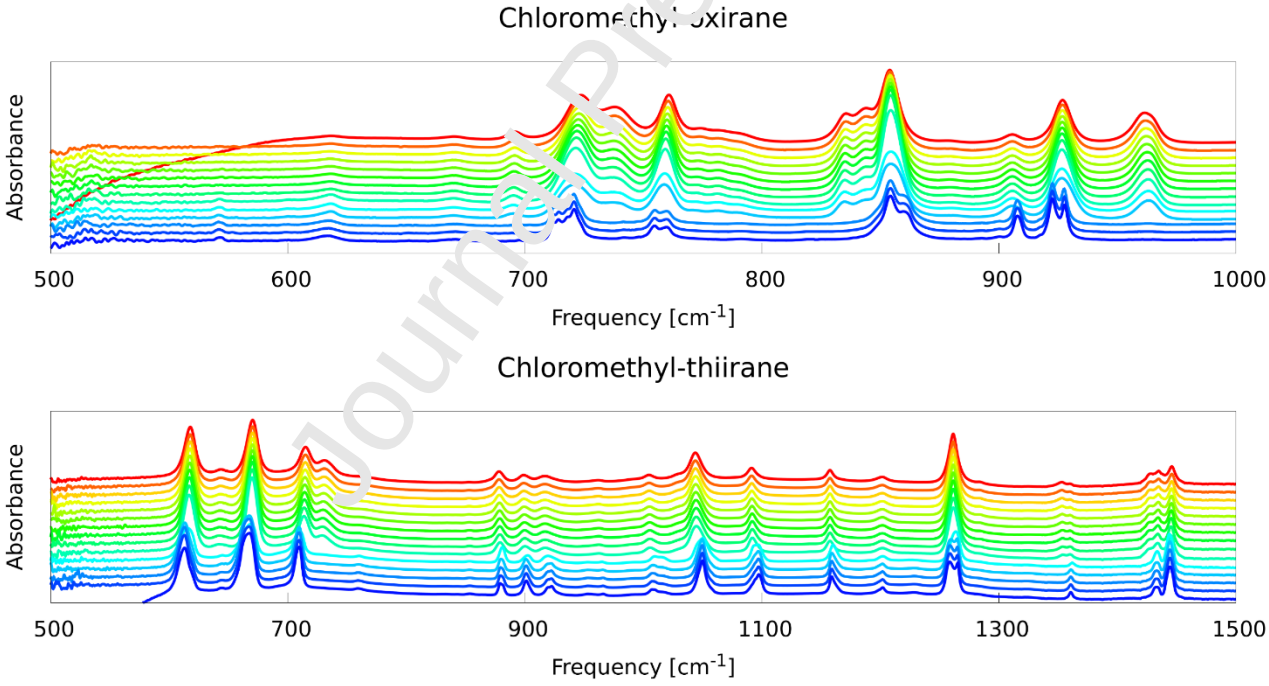

Figure 5b MIR spectrum details (blue T_{min}, red T_{max}).

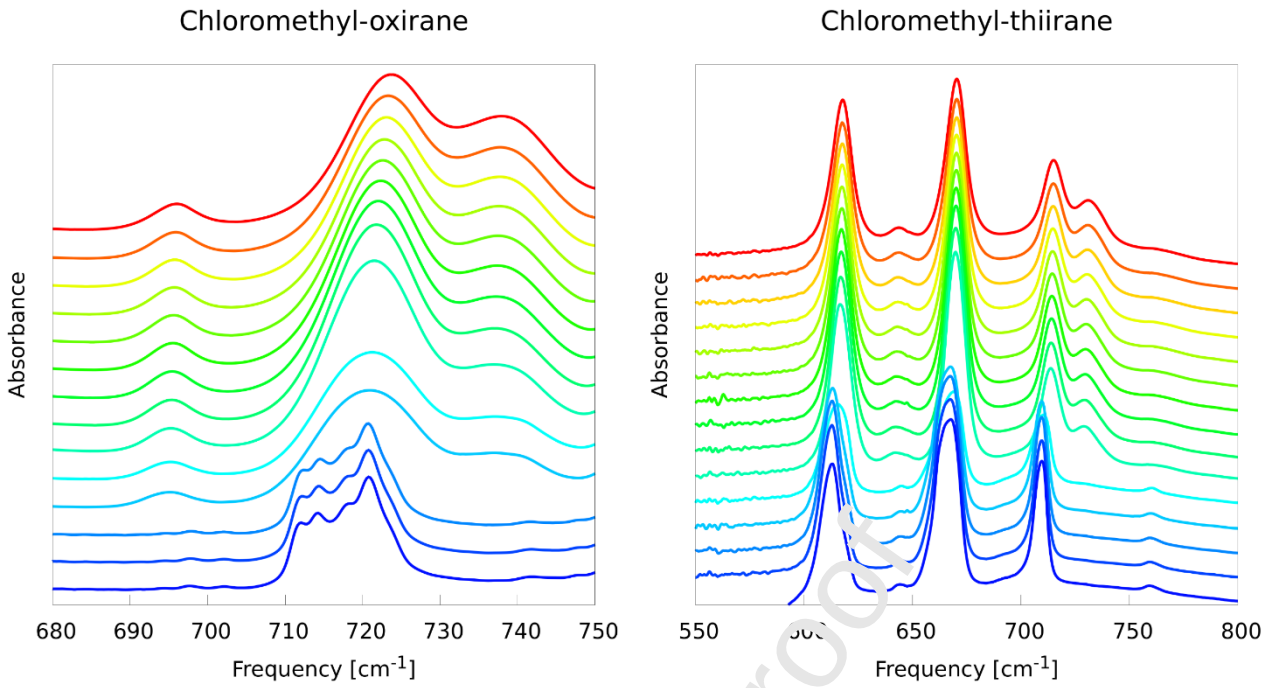

Figure 6 MIR spectrum details (blue Tmin, red Tmax)

At this point of the work, the determination from the present FTIR measures at variable temperatures of conformational ΔH values for the two liquids has to be considered.
The infrared spectrum of chloromethyl-oxirane in the frequency range between 50 and 1000 cm^{-1} measured on cooling between 300 and 150 K is reported in **Figures 5a** and **5b.** It is also of particular interest to examine the spectral regions 680-750 cm^{-1} (see **Figure 6**).

Several absorption lines are observable and by means of the comparison with calculations, some of them were clearly attributed to the conformers *gauche-1, gauche-2* and *cis*. In particular, below 650 cm^{-1}, the line at 518 cm^{-1} is attributed to *cis* conformer, the line at 443 cm^{-1} to *gauche-1* and the lines at 363 and 225 cm-1 are both attributed to *gauche-2*. Similarly, between 1000 and 650 cm^{-1}, one can observe at 695 cm^{-1} another absorption due to the *cis* conformer, at 723, 860, 910 and 930 cm^{-1} lines due to the *gauche-1* conformer and at 738, and 845 cm^{-1} lines due to the *gauche-2* conformer. At 760 cm^{-1} at 300 K there is the superposition of contributions coming both from the *gauche-1* and *cis* state. On cooling, the lines become narrower but at around 190 K the intensity of several lines, and in particular of those ones attributed to the *cis* and *gauche-2* conformers strongly decreases (*i.e.* the lines at 225, 518 and 740 cm^{-1}) and on further cooling at 180 K disappears. As largely discussed, the concomitant increase of the intensity of lines attributed to the *gauche-1*conformer suggests the occurring of a phase transition towards a solid state, in agreement with previous literature reporting that the solid state is mainly characterized by the presence of the more stable *gauche-1* conformer [1]. As already reported in the previous sections, one observes an amorphous state between the liquid and the solid.
More indications about the liquid phase can be obtained by a quantitative analysis of the IR spectrum, which provides a detailed picture of the temperature evolution of the conformers in the samples [23-31].
Indeed, the ratio of the intensities $r_{1,2}$ of the lines attributable to two different conformers is proportional to their relative concentration:
$r_{1,2} = \frac{I_1 x}{I_{2y}} = \frac{[C1]}{[C2]}$where I_x indicates the integrated infrared intensity of the band centered at wavenumber *x* [25-26, 28, 30-31] being attributed to a specific conformer, after subtraction of the

background. It can be observed that in the liquid state the relative concentration of two conformers follows the Boltzmann law, which leads to the Van't Hoff relation

$\ln(r_{12}) = -\frac{\Delta H_{1,2}}{RT} + \frac{\Delta S_{1,2}}{R}$ where $\Delta H_{1,2}$ and $\Delta S_{1,2}$ are the enthalpy and entropy differences between the two conformers. In the present case, in order to calculate the relative concentration of each couple of conformers, well defined lines which could be unambiguously attributed were chosen for each. In particular, the analysis was performed calculating several ratios with two groups of lines.

For the first group of lines, the peaks at 443, 225 and 518 cm^{-1}, respectively attributed to *gauche-1*, (G1), *gauche-2,* (G2) and *cis* conformers were employed.

The intensities were obtained by fitting each line with a Lorentzian function after subtracting a linear background. The plot of ln(*r*) *vs* 1/*T* for all the ratios are reported in **Figure 7**.

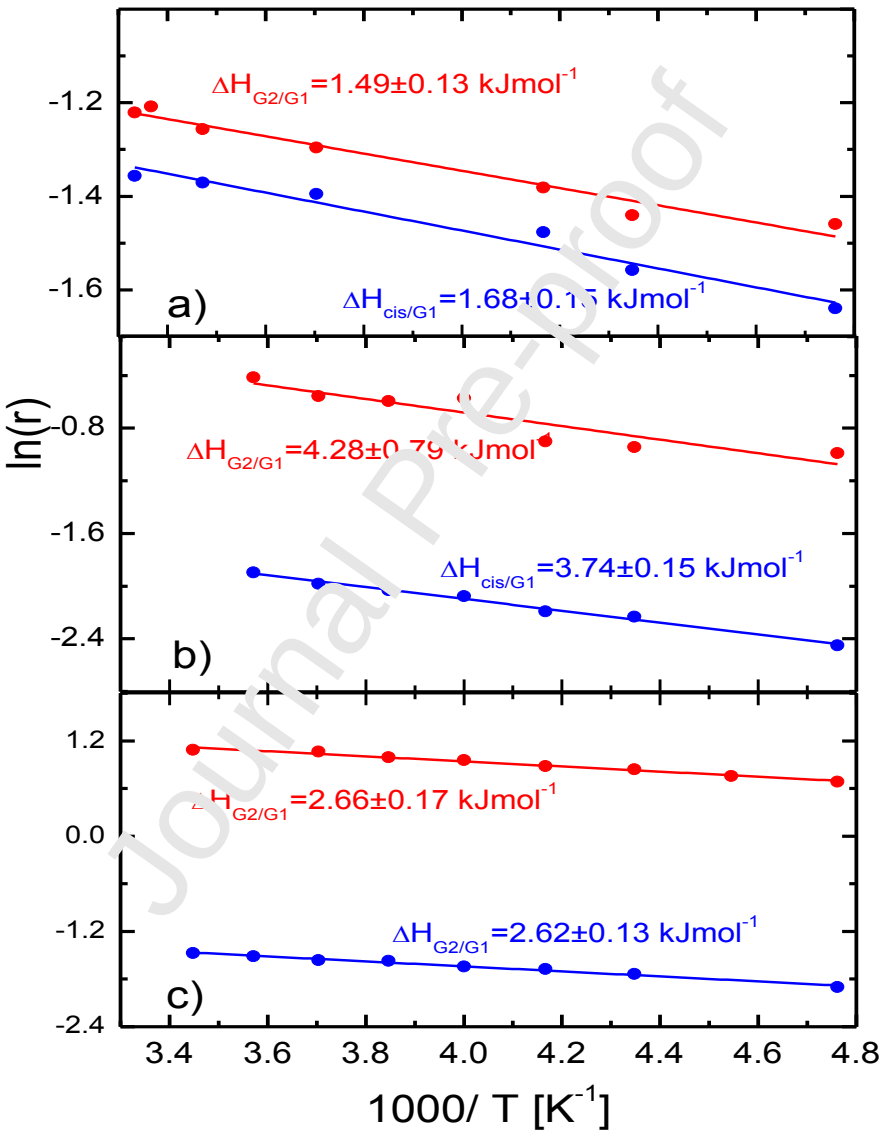

Figure 7 Temperature dependence of the logarithm of the ratio of the intensities of the bands due to the different conformers of chloromethyl-oxirane (panel a and b, see text for details on the considered bands) and of chloromethyl-thiirane (panel c), together with the best fit curves. In particular, in the panel ***a)*** *ratios were calculated considering lines at 443 (G1), 225 (G2) and 518 cm^{-1}* (cis)*, in panel* ***b)*** *lines at 723 (G1), 738 (G2) and 695 cm^{-1},* (cis)*; in panel* ***c)*** *considering lines at 410 (G1) and 385 cm^{-1} (G2) for red points; lines at 640 and 735 cm^{-1} (G1) and lines at 610, 670 and 715 cm^{-1} (G2) for blue points.*

The treatment of the first group of data (panel **a)** of **Figure 7**) produces for the conformational equilibria the corresponding enthalpy changes:

gauche-2↔*gauche-1* ΔH= 125 ± 11 cm^{-1} (1.49 ± 0.13 kJ·mol^{-1})
gauche-1↔*cis* ΔH= 140 ± 13 cm^{-1} (1.68 ± 0.15 kJ·mol^{-1})

The second group of frequencies takes into consideration the lines at 723, 738 and 695 cm^{-1}, respectively attributed to *gauche-1*, *gauche-2* and *cis* conformers.
The intensities are obtained by the fit realized adding three Gaussian functions after subtracting a linear background. The plots of ln(*r*) *vs* 1/*T* are reported in panel **b)** of **Figure 7.**
From the treatment of these data, the following enthalpy changes were obtained for the conformational equilibria reported below:

gauche-1↔*gauche-2* ΔH =358 ± 11 cm^{-1} (4.28 ± 0.79 kJ·mol^{-1})
gauche-1↔*cis* ΔH =313 ± 13 cm^{-1} (3.74 ± 0.15 kJ·mol^{-1})

The ΔH values from the two groups of lines are different, but the second group is in good agreement with those found previously by Durig [1] in the same frequency range. It must be noted that the analysis in the FIR range was firstly performed here, in this case we have to fit the three lines separately due to the wide range in which they occur contrarily to the procedure for the MIR range. Therefore, the latter value should be more reliable. Another consideration is that the experimental ΔH values for the liquid state conformational equilibria are quite higher than the corresponding ones determined though the same procedure in liquid Xe solutions [1] and for this reason the gas phase conversion between the *gauche* forms is energetically less favored in the liquid where the estimated barriers are higher.
These results corroborate the conclusions reached from static and dynamic *ab initio* calculations, namely that the *gauche-1* conformer is the most stable (and therefore most populated) in the liquid phase. The ΔH values for the *gauche-1*↔*gauche-2* and *cis*↔*gauche-1* conformational equilibria occurring in the liquid are well comparable within the errors, in agreement with those previously reported by literature [1]. Moreover, these values are all positive, confirming an increase of the *gauche-2* and *cis* concentration with temperature in the liquid phase.
The agreement with theoretical enthalpies estimated through G4MP2 approach at 298 K is partial: a remarkable matching (fully within experimental error) can in fact be obtained for the *gauche-1*↔*cis* conversion (318 cm^{-1} with respect to the 313 ± 13 cm^{-1} experimental value) but, for the *gauche-1*↔*gauche-2* interconversion, the calculated value is less than half of the experimental one (134 with respect to 358 ± 11 cm^{-1}).
The infrared spectrum of chloromethyl-thiirane in the frequency range between 50 and 1500 cm^{-1} measured on cooling between 300 and 160 K is also reported in **Figure 5** and the frequency range 550 – 800 cm^{-1} is shown in **Figure 6**. Several absorption lines are observable and by means of the comparison with calculation, some of them can be clearly attributed to the various conformers. In particular, below 450 cm^{-1} there are two well separated lines at 385 and 410 cm^{-1}, which are respectively due to the *gauche-1* and *gauche-2* conformers. Other signals at 640, 735, 920 and 1050 cm^{-1} can be attributed to the *gauche-1* conformer, while those at 610, 670, 715, 880, 900, 1010, 1160,1200, 1265, 1430 and 1440 $cm^{-1}$are due to *gauche-2* conformer. In the measured spectrum no observed line can be attributed to the *cis* conformer, thus confirming that the liquid state is a mixture of the two *gauche* rotamers.
As already discussed in the previous sections, the passage through an amorphous phase is observed inthe spectra, followed by the crystallization below 200 K. More indications about the liquid phase can be obtained by a quantitative analysis of the IR spectrum, which provides a

detailed picture of the temperature evolution of the conformers in the samples [24– 31].

For chloromethyl-thiirane we can select two groups of well detectable lines whose analysis can provide the ratio between the *gauche-1* and *gauche-2* conformers. In particular, we carried out a detailed analysis in the following ranges where the different contributions were well separated: around 400 cm^{-1}, with lines at 385 and 410 cm^{-1}, respectively due to the *gauche-1* and *gauche-2* conformer and between 550 and 700 cm^{-1}, where we can assign the lines at 640 and 735 cm^{-1} to the *gauche-1* conformer and the lines at 610, 670 and 715 cm^{-1} to the *gauche-2* conformers. The relative concentration between the two conformers were calculated as:

$$r_{G_2,G_1} = \frac{I_{G_1}}{I_{G_2}} = \frac{I_{385}}{I_{410}};\ r_{G_2,G_1} = \frac{I_{G_1}}{I_{G_2}} = \frac{I_{640}+I_{735}}{I_{610}+I_{670}+I_{715}}$$

The intensities are obtained by the fit realized considering two (around 400 cm^{-1}) or five (between 550 and 700 cm^{-1}) Gaussian functions after subtracting a linear background. The plot of ln(*r*)*vs* $1/T$ for the above ratios are reported in panel **c)** of **Figure 7.**

From these linear regressions one reaches the following ΔH values for the conformational equilibrium of chloromethyl-thiirane in the liquid state *gauche-2*↔*gauche-1*:ΔH = 222 ± 14 cm^{-1} (2.66 ± 0.17 kJ·mol^{-1}) using the first group of data and ΔH= 219 ± 11 cm^{-1} (2.62 ± 0.13 kJ·mol^{-1}) using the second group of frequencies. The obtained values (coincident within the errors) are evidently positive and thus confirm that the *gauche-2* conformer is the most stable and therefore the most abundant component of the liquid phase and also suggest an increase of the *gauche-1* concentration with the temperature. These ΔH values are meaningfully larger than the corresponding values reported in literature [2] determined in low temperature xenon solution, that is for the gas phase (105 ± 15 cm^{-1} (1.26 ± 0.18 kJ·mol^{-1})). These differences are explainable as consequence of different polarity of the two conformers. In addition, the less stable conformer *gauche-1* increases its dipole in the liquid phase (see **Table 2** of the Supporting Information) enhancing the role of intermolecular interactions. Even in this case, agreement with calculated data is not perfect, being the theoretical ΔH for the *gauche-2*↔*gauche-1* equilibrium in liquid phase equal to 164 cm^{-1}.

At last, in order to investigate the effect of the addition of a solvent on the conformer population we also measured the FTIR spectrum at room temperature of mixed systems obtained by adding an apolar (CCl_4) or polar (DMSO or H_2O) solvent to the starting chloromethyl-oxirane or chloromethyl-thiirane liquid sample, and the results are given in **Figures 8a** and **8b**.

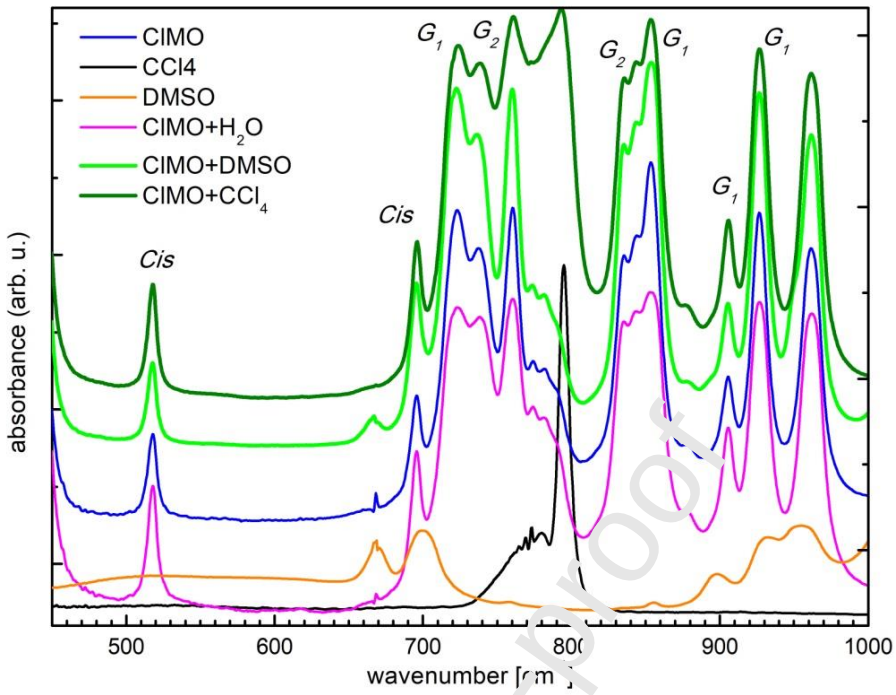

Figure 8a Comparison of the IR spectra of chloromethyl-oxirane, with its mixtures with DMSO, CCl_4 and H_2O. For comparison also the spectra of the solvents are reported.

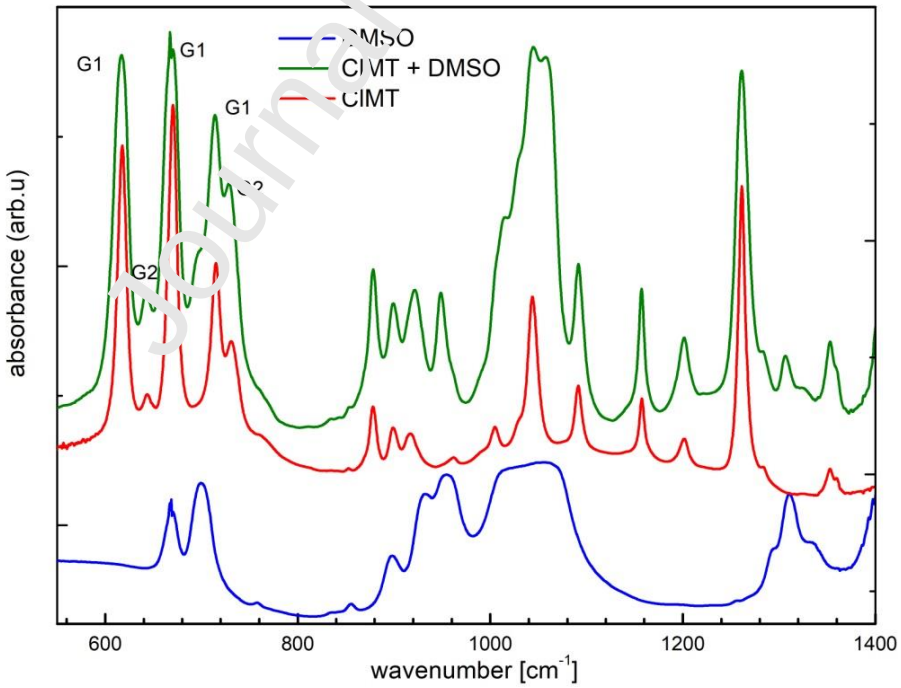

Figure 8b Comparison of the IR spectra of chloromethyl-thiirane with its mixture with DMSO. For comparison also the spectra of the solvent are reported.

As a reference, the IR spectrum measured in the same conditions on the pure solvents is also reported in both figures. The addition of the polar DMSO solvent induced an increase of the intensity of lines attributed to the more stable *gauche-1* conformer, while the presence of the apolar CCl_4 lowers this intensity, thus suggesting a decrease of the *gauche-1*population in the liquid.

Concerning chloromethyl-thiirane, the addition of the polar DMSO solvent seems to induce a slight increase in the relative intensity of lines attributed to the *gauche-1* conformer. Such an effect is however less valuable than for chloromethyl-oxirane, not permitting an inversion of the stability order between the conformers, as summarized in **Table 3**. For this purpose, it has to be reminded that the behavior of some bands of chloromethyl-thiirane (more precisely those measured between 770 and 570 cm^{-1}) under the influence of the environment was observed in a former study carried out in vapor, liquid, acetone and carbon disulfide [32] revealing in advance what is now supported by calculations as well as by FTIR studies. The spectra in CCl_4 were not of good quality and therefore are not shown.

CONCLUSIONS

The calculations considered in the whole, spanning from stability, conformational populations and infrared spectroscopy, would seem to have reached satisfactory results. The energy minima are well localized and deep and the interconversion from a conformer to another is prevented enough in vapor and liquid phase, since at ordinary temperature the energy barriers separating them are higher than kT. The stabilization of one gauche species occurring at low temperature in the crystalline forms (*gauche-1* for chloromethyl-oxirane and *gauche-2* for chloromethyl-thiirane) only depends on the effect of polarity for the former compound and on the net prevalence of steric effect for the latter molecule. The effect of the chemical surrounding computationally simulated through the PCM approximation would seem to produce valuable conclusions confirmed by FTIR measures. Adopting that strategy, even in the simplest version of the PCM method (without making explicit the chemical nature of the solvation shell at molecular level), we were able to correctly predict how polarity of the continuum medium might exert its influence on the stability and the conformational population of the most stable rotamers, as experimentally observed in the FTIR spectra measured in different conditions. AIMD computations were also of some interest because provided results consistent with the other theoretical approaches. These further computations confirm the consequences of polarity of the medium on the conformational equilibria and of temperature, although qualitatively. The latter simulations, within the limits of the approximations adopted, suggest that sample cooling favors the most polar conformer for chloromethyl-oxirane and the less polar one, but also less sterically hindered, for chloromethyl-thiirane as actually observed.

ACKNOWLEDGEMENTS

We wish to thank P. Roy and J.-B. Brubach for assistance at the AILES beamline of Synchrotron Soleil during beamtime #20170928 and #20190321. The beamtimes received funding from the European Union's Horizon 2020 Research and Innovation programme under Grant Agreement No 730872 (CALIPSOplus). LG acknowledges support from Regione Lazio, through Progetto di Ricerca 85-2017-15125 according to L. R. 13/08.

CPU computing time was granted by the "Department of Excellence-2018" Program (Dipartimenti di Eccellenza) of the Italian Ministry of Research, DIBAF-Department of University of Tuscia, Project "Landscape 4.0 - food, wellbeing and environment" (Prof. Nico Sanna) and from Cagliari

University computing clusters (Prof. Francesca Mocci).

SUPPORTING INFORMATION

Table 2-2 Energetic profiles[(a)] of chloromethyl-oxirane and chloromethyl-thiirane in different solvents

Table 3 MP4(SDTQ)/6-311++G(3df,3pd)//B3LYP/6-311++G(3df, 3pd) energy differences (cm^{-1}) calculated between the stationary points in different environments

Table 4 Temperature dependence of the conformational populations

Table 5- B3LYP/6-311++G(3df,3pd) anharmonic frequencies (cm^{-1}) of chloromethyl-oxirane and chloromethyl-thiirane in different solvents

Table 6 -7 Chloromethyl-oxirane B3LYP/6-311++G(3df,3pd) harmonic and anharmonic frequencies and intensities of chloromethyl-oxirane and chloromethyl-thiirane in different solvents

Table 8 Conformer population of the pure liquids at low temperature from AIMD.

REFERENCES

[1] M. J. Lee, S. W. Hur, J. R. Durig, Conformational stability, vibrational assignments, and normal coordinate analysis from FT-IR spectra of xenon solutions and ab initio calculations of epichlorohydrin, J. Mol. Struct. 444, (1998) 99-113, https://doi.org/10.1016/S0022-2860(97)00344-X

[2] J. R. Durig, B. R. Drew, J. A. Shoup, C. J. Wurrey, Conformational stability determination of chloromethyl thiirane from variable temperature FT-IR studies of rare gas solutions, structural parameters, and ab initio calculations, J. Mol. Struct.569 (2001)195-212,https://doi.org/10.1016/S0022-2860(01)00430-6

[3] L. Gontrani, S. Nunziante Cesaro, S. Stranges, L. Bencivenni, A. Pieretti, FTIR spectra and density functional theory P.E.D. assignments of oxiranes in Ar matrix at 12 K Spectrochim Acta A Mol Biomol Spectrosc, 120 (2014) 558–567, https://doi.org/10.1016/j.saa.2013.12.005

[4] M. Campetella, L. Bencivenni, R. Caminiti, C. Zazza , S. Di Trapani , A. Martino, L. Gontrani, Chloromethyl-oxirane and chloromethyl-thiirane in liquid phase: A joint experimental and quantum chemical study, Chem. Phys. 473 (2016) 24–31, https://doi.org/10.1016/j.chemphys.2016.03.027

[5] P. Roy, M. Guidi Cestelli, A. Nucara, O. Marcouille, P. Calvani, P. Giura, A. Paolone, Y.-L. Mathis, A. Gerschel, Spectral Distribution of Infrared Synchrotron Radiation by an Insertion Device and Its Edges: A Comparison Between Experimental and Simulated Spectra. Phys. Rev. Lett. 84 (2000), 483−486, https://doi.org/10.1103/PhysRevLett.84.483

[6] P. Roy, J.-B. Brubach, P. Calvani, G. De Marzi, A. Filabozzi, A. Gerschel, P. Giura, S. Lupi, O. Marcouille, A. Mermet,A. Nucara, J. Orphale, A. Paolone, M.Vervloete . Infrared Synchrotron Radiation: from the Production to the Spectroscopic and Microscopic Applications. Nucl. Instrum. Methods Phys. Res. Sect. A 2001, 426, 467-468, https://doi.org/10.1016/S0168-9002(01)00349-7

[7] Gaussian 16, Revision C.01, M. J. Frisch, G. W. Trucks, H. B. Schlegel, G. E. Scuseria, M. A.

Robb, J. R. Cheeseman, G. Scalmani, V. Barone, G. A. Petersson, H. Nakatsuji, X. Li, M. Caricato, A. V. Marenich, J. Bloino, B. G. Janesko, R. Gomperts, B. Mennucci, H. P. Hratchian, J. V. Ortiz, A. F. Izmaylov, J. L. Sonnenberg, D. Williams-Young, F. Ding, F. Lipparini, F. Egidi, J. Goings, B. Peng, A. Petrone, T. Henderson, D. Ranasinghe, V. G. Zakrzewski, J. Gao, N. Rega, G. Zheng, W. Liang, M. Hada, M. Ehara, K. Toyota, R. Fukuda, J. Hasegawa, M. Ishida, T. Nakajima, Y. Honda, O. Kitao, H. Nakai, T. Vreven, K. Throssell, J. A. Montgomery, Jr., J. E. Peralta, F. Ogliaro, M. J. Bearpark, J. J. Heyd, E. N. Brothers, K. N. Kudin, V. N. Staroverov, T. A. Keith, R. Kobayashi, J. Normand, K. Raghavachari, A. P. Rendell, J. C. Burant, S. S. Iyengar, J. Tomasi, M. Cossi, J. M. Millam, M. Klene, C. Adamo, R. Cammi, J. W. Ochterski, R. L. Martin, K. Morokuma, O. Farkas, J. B. Foresman, and D. J. Fox, Gaussian, Inc., Wallingford CT, 2016.

[8] J. Tomasi, B. Mennucci, R. Cammi, Quantum Mechanical Continuum Solvation Models, Chem. Rev., 105 (8) (2005) 2999-3093, https://doi.org/10.1021/cr9904009

[9] Static Dielectric Constants of Pure Liquids and Binary Liquid Mixtures, C. Wohlahrt, (O. Madelung), Springer – Verlag (2008)

Author Contributions

LG, FC, AP and OP conceived the idea, MC and LG performed AIMD calculations, FC performed static ab initio calculations, AP and OP carried out FTIR measurements. LG, FC AP, OP and MC wrote the manuscript, LG and FR supervised the project. All authors discussed the results and contributed to the final revision of the manuscript.

Declaration of interests

☒ The authors declare that they have no known competing financial interests or personal relationships that could have appeared to influence the work reported in this paper.

☐The authors declare the following financial interests/personal relationships which may be considered as potential competing interests:

Graphical abstract

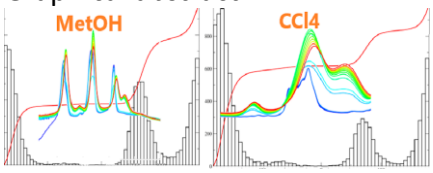

Highlights

- Conformational landscape of chloromethyl-oxirane and chloromethyl-thiirane is investigated with infrared spectroscopy and computational techniques
- Spectra of the two liquids were taken at room temperature and upon cooling below melting temperature, up to 160K
- The oxirane compound shows the presence of two difference conformers of different polarity in the liquid, with a negligible trace of cis form, whereas in thiirane the apolar form Gauche-2 is dominant
- Conformational equilibria vary markedly with the polarity of the environment. The relative population of polar conformers increases in methanol and DMSO, whereas apolar forms prevail in apolar solvents

References

[10] L. Tanzi, F. Ramondo, R. Caminiti, M. Campetella, A. Di Luca, L. Gontrani, Structural Studies on Choline-Carboxylate Bio-Ionic Liquids by X-Ray Scattering and Molecular DynamicsJ. Chem. Phys. 143(11), (2015) 114506, https://doi.org/10.1063/1.4931031

[11] M. Campetella, D. Chillura Martino, E. Scarpellini, L. Gontrani, Low-Q peak in X-ray patterns of choline-phenylalanine and -homophenylalanine: A combined effect of chain and stackingChem. Phys. Lett. 660, (2016) 99-101 https://doi.org/10.1016/j.cplett.2016.08.015

[12] M. Campetella, S. De Santis, R. Caminiti, P. Ballirano, C. Sadun, L. Tanzi, L. Gontrani, Is a medium-range order pre-peak possible for ionic liquids without an aliphatic chain? RSC Adv. 5(63) (2015)50938-50941, https://doi.org/10.1039/C5RA07567J

[13] M. Campetella, M. Montagna, L. Gontrani, E. Scarpellini, F. Bodo, Unexpected proton mobility in the bulk phase of cholinium-based ionic liquids: new insights from theoretical calculationsPhys. Chem. Chem. Phys. 19 (2017) 11869-11880, https://doi.org/10.1039/C7CP01050H

[14] M. Campetella, M. Macchiagodena, L. Gontrani, B. Kirchner, Effect of alkyl chain length in protic ionic liquids: an AIMD perspective, Mol. Phys. 115 (13) (2017) https://doi.org/10.1080/00268976.2017.1308027 1582-1589

[15] R. Salomon-Ferrer, D. A. Case, R.C. Walker, An overview of the Amber biomolecular simulation package, WIREs Comput. Mol. Sci. 3(2) (2013)198-210, https://doi.org/10.1002/wcms.1121.

[16] J.Wang, R. M. Wolf, J.W.Caldwell, P.A.Kollman, D.A.Case,Development and testing of a general amber force field, J. Comput. Chem. 25(9), (2004)1157-1174, https://doi.org/10.1002/jcc.20035

[17] J. Hutter, M. Iannuzzi, F. Schiffmann, J. VandeVondele, cp2k: atomistic simulations of condensed matter systems, WIREs Comput. Mol. Sci. 4(1), (2014)15-25, https://doi.org/10.1002/wcms.1159

[18] J. VandeVondele, M. Krack, F. Mohamed, M. Parrinello, T. Chassaing, and J. Hutter, Quickstep: Fast and accurate density functional calculations using a mixed Gaussian and plane waves approach, Comput. Phys. Commun. 167(2), (2005)103-128 https://doi.org/10.1016/j.cpc.2004.12.014

[19] J.P. Perdew, K. Burke, and M. Ernzerhof,,Generalized Gradient Approximation Made SimplePhys. Rev. Lett. 77(18), (1996)3865, https://journals.aps.org/prl/abstract/10.1103/PhysRevLett.77.3865

[20] S. Grimme, Semiempirical GGA-type Density Functional Constructed With a Long-Range Dispersion CorrectionJ. Comput. Chem. 27(15) (2006)1787-1799, https://doi.org/10.1002/jcc.20495

[21] J. VandeVondele, J. Hutter, Gaussian basis sets for accurate calculations on molecular systems in gas and condensed phases, J. Chem. Phys. 127(11) (2007)114105, https://doi.org/10.1063/1.2770708

[22] S. Goedecker, M. Teter, J. Hutter, Separable dual-space Gaussian pseudopotentialsPhys. Rev. B 54(3),1703 (1996), https://doi.org/10.1103/PhysRevB.54.1703

[23] F. M. Vitucci, D. Manzo, M. A. Navarra, O. Palumbo, F. Trequattrini, S. Panero, P. Bruni, F. Croce, A. Paolone, Low-Temperature Phase Transitions of 1-Butyl-1-methylpyrrolidinium Bis(trifluoromethanesulfonyl)imide Swelling a Polyvinylidenefluoride Electrospun Membrane, J. Phys. Chem. C 118 (2014) 5749-5755, https://doi.org/10.1021/jp500668b

[24] F. M. Vitucci, F. Trequattrini, O. Palumbo, J.-B. Brubach, P. Roy, A. Paolone, Infrared Spectra of Bis(trifluoromethanesulfonyl)imide Based Ionic Liquids: Experiments and Ab-initio Simulations. Vib. Spec. 74 (2014) 81–87, https://doi.org/10.1016/j.vibspec.2014.07.014

[25] F. M. Vitucci, F. Trequattrini, O. Palumbo, J.-B. Brubach, P. Roy, A. Paolone, A. Stabilization of Different Conformers of Bis(trifluoromethanesulfonyl)imide Anion in Ammonium-Based Ionic Liquids at Low Temperatures. J. Phys. Chem. A 118 (2014) 8758−8764, https://doi.org/10.1021/jp504833e

[26] O. Palumbo, F. Trequattrini, F. M. Vitucci, M. A. Navarra, S. Panero, A. Paolone, An Infrared Spectroscopy Study of the Conformational Evolution of the Bis(trifluoromethanesulfonyl)imide Ion in the Liquid and in the Glass State. Adv. Cond. Matter. Phys. 2015, (2015), 176067 https://doi.org/10.1155/2015/176067

[27] F. M. Vitucci, O. Palumbo, F. Trequattrini, J.-B. Brubach, P. Roy, I. Meschini, F. Croce, A. Paolone, Interaction of 1-Butyl-1- methylpyrrolidiniumBis(trifluoromethanesulfonyl)imide with an Electrospun PVdF Membrane: Temperature Dependence of the Concentration of the Anion Conformers. J. Chem. Phys. 143 (2015) 094707, https://doi.org/10.1063/1.4929986

[28] F. Capitani, S. Gatto, P. Postorino, O. Palumbo, F. Trequattrini, F.; M. Deutsch, J.-B. Brubach, P. Roy, A. Paolone, The Complex Dance of the Two Conformers of Bis(trifluoromethanesulfonyl)imide as a Function of Pressure and Temperature. J. Phys. Chem. B 120 (2016) 1312−1318, https://doi.org/10.1021/acs.jpcb.5b12537

[29] F. Capitani, F. Trequattrini, O. Palumbo, A. Paolone, P. Postorino, Phase Transitions of PYR14-TFSI as a Function of Pressure and Temperature: the Competition Between Smaller Volume and Lower Energy Conformer, J. Phys. Chem. B 120 (2016) 2921-2928, https://doi.org/10.1021/acs.jpcb.5b12667

[30] O. Palumbo, F. Trequattrini, M. A. Navarra, J.-B. Brubach, P. Roy, A. Paolone,.Tailoring the Physical Properties of the Mixtures of Ionic liquids: a Microscopic Point of View. Phys. Chem. Chem. Phys. 19 (2017) 8322-89329, https://doi.org/10.1039/C7CP00850C

[31] O. Palumbo, F. Trequattrini, G. B. Appetecchi, A. Paolone, The Influence of the Alkyl Chain Length on the Microscopic Configurations of the Anion in the Crystalline Phases of PYR_{1A} TFSI. J. Phys. Chem. C, 121(21) (2017), 11129–11135, https://doi.org/10.1021/acs.jpcc.7b02365

[32] C. J. Wurrey, Y. Y. Chen, F. G. Rojas, P. M. Green, A. J. Holder, R. C. Kenton, V. F. Kalinsky, M. T. Ho, C. F. Su, R. L. Cook, Vibrational and rotational spectra and conformational behavior of (chloromethyl)thiirane, Spectrochim. Acta 50 A (1994) 481-492, https://doi.org/10.1016/0584-8539(94)80163-0

[33] M. Campetella, L. Gontrani, E. Bodo, F. Ceccacci, F. Cesare Marincola, R. Caminiti, Conformational isomerisms and nano-aggregation in substituted alkylammonium nitrates ionic liquids: An x-ray and computational study of 2-methoxyethylammonium nitrate, J. Chem. Phys. 138(18), (2013) 184506, https://aip.scitation.org/doi/10.1063/1.4803799

[34] G. Prampolini, M. Campetella, N. De Mitri, P. R. Livotto, I. Cacelli, Systematic and Automated Development of Quantum Mechanically Derived Force Fields: The Challenging Case of Halogenated Hydrocarbons, J. Chem. Theor. Comput. 12(11), (2016). 5525-5540 https://pubs.acs.org/doi/10.1021/acs.jctc.6b00705

[35] O. Andreussi, I. G. Prandi, M. Campetella, G. Prampolini, B. Mennucci, Classical Force Fields Tailored for QM Applications: Is It Really a Feasible Strategy? J. Chem. Theory Comput. 13 (2017) 4636-4648, https://pubs.acs.org/doi/10.1021/acs.jctc.7b00777